Review

Advances in GPCR-Targeted PET Radiotracer Patents (2020–2025)

Rebecca Ferrisi * , Clara Mocchetti , Alessia Cazzaniga , Marco De Amici , Claudio Papotto , Clelia Dallanoce

Posted Date: 9 April 2026

doi: 10.20944/preprints202604.0617.v1

Keywords: positron emission tomography; G protein-coupled receptors; radioligands; GPCR-targeted tracers; molecular imaging; tracer development

 doi:10.20944/preprints202604.0617.v1

Review

Advances in GPCR-Targeted PET Radiotracer Patents (2020–2025)

Rebecca Ferrisi [1,*], Clara Mocchetti [1], Alessia Cazzaniga [1], Marco De Amici [1], Claudio Papotto [2], Clelia Dallanoce [1]

[1] Department of Pharmaceutical Sciences, Medicinal Chemistry Section "Pietro Pratesi", University of Milan, Via L. Mangiagalli 25, Milan 20133, Italy

[2] Tecnomed Foundation, University of Milan-Bicocca, Via G. Pergolesi 33, Monza 20900, Italy

* Correspondence: rebecca.ferrisi@unimi.it

Abstract

Background: Positron emission tomography (PET) is a molecular imaging technique that exploits the β^+ decay of selected radionuclides to enable non-invasive *in vivo* investigation of biochemical and physiological processes, including early and subclinical disease alterations. Radiotracers are designed to bind specific molecular targets with high affinity and selectivity. Among the targets to which PET devotes increasing attention are G protein-coupled receptors (GPCRs)—the largest class of transmembrane receptors—which orchestrate a wide spectrum of biological outcomes and are widely implicated in human disease. **Objectives:** This review analyzes patents published between 2020 and 2025 focusing on GPCR-targeted PET radiotracers, highlighting design strategies, radionuclide selection, and translational perspectives across oncology, central nervous system (CNS) disorders, and inflammatory diseases. **Results:** Patent activity shows that most GPCR-targeted PET tracers are derived from validated ligands adapted for imaging while preserving affinity and selectivity. Oncology patents mainly favor peptide-based or modular metal–chelator platforms enabling radionuclide flexibility and theranostic extension, whereas CNS tracers rely on drug-like small molecules optimized under strict ADME and blood–brain barrier constraints. Increasing emphasis on non-orthosteric, function-sensitive, and dual-targeting approaches reflects a shift toward interrogating GPCR signaling states, while inflammatory indications remain comparatively underrepresented despite clear biological foundations. **Conclusions:** Current patent trends consolidate GPCR-targeted PET tracers as well-established diagnostic tools while progressively expanding their clinical utility, both as platforms supporting translational research—informing mechanistic insight and drug development—and as components of emerging theranostic strategies across multiple disease areas.

Keywords: positron emission tomography; G protein-coupled receptors; radioligands; GPCR-targeted tracers; molecular imaging; tracer development

1. Introduction

Positron emission tomography (PET) is an advanced imaging technique in nuclear medicine that enables the study of physiological and pathophysiological processes in various organs of the body. It involves the administration of a *radiopharmaceutical*— a chemical entity, just like other medicinal molecules or xenobiotics in general, containing one radioactive atom—that accumulates in specific areas of the body based on its biochemical properties. The isotope within the radiopharmaceutical undergoes β^+ decay, emitting a positron that subsequently interacts with a nearby electron in the surrounding tissue. This interaction results in an annihilation event, producing two 511-keV photons

 doi:10.20944/preprints202604.0617.v1

emitted in opposite trajectories, which are detected by a scintillator in the scanning device (Figure 1). Sophisticated computational algorithms then reconstruct the photon trajectories to create a three-dimensional image, providing a quantitative map of radiotracer uptake in specific tissues. This enables the *in vivo* assessment of biochemical and physiological processes, which, in cases of aberrations, may occur prior to the appearance of macroscopic anatomical signs of a disease [1,2].

A variety of radionuclides is used in nuclear medicine. This broad family can be divided into mainly therapeutic and diagnostic nuclides. Therapeutic radionuclides are primarily particle emitters (α, β^- and, in some cases, Auger electrons) used in targeted radionuclide therapy (e.g. ^{225}Ac, ^{32}P, ^{177}Lu, ^{131}I). Diagnostic nuclides include γ-emitters (for scintigraphy and SPECT) and positron-emitters (PET). Notably, some radionuclides (e.g., ^{177}Lu and ^{131}I) show both therapeutic particle emissions and useful γ emissions, enabling post-therapy imaging/dosimetry.

In the context of PET, fluorine-18 (^{18}F) and carbon-11 (^{11}C) are among the most widely used β^+-emitting radionuclides (Table 1). ^{18}F offers several advantages over other PET radionuclides, including a short positron range (<1 mm), which enables high-resolution image acquisition, a favorable decay profile (97% positron emission and 3% electron capture), and an optimal physical half-life of 109.8 min, allowing distribution to satellite facilities without an on-site cyclotron [3]. Although ^{18}F is highly competitive and often preferred for peptides and small biomolecules, it is not the first choice radionuclide for larger biomolecules such as antibodies, nanobodies, proteins, or oligonucleotides, where longer-lived radionuclides like ^{89}Zr (78 h) and ^{64}Cu (12.7 h) are more suitable to match their slower pharmacokinetics and enable imaging at 24–72 h post-injection [4]. ^{18}F is by far the most widely used radionuclide in oncology, primarily owing to 2-deoxy-2-[^{18}F]fluoroglucose or [^{18}F]Fluorodeoxyglucose ([^{18}F]FDG), a glucose analogue bearing a bioisosteric substitution of the hydroxyl group at the 2-position with ^{18}F, which represents the universal standard for oncologic PET imaging [5]. ^{11}C presents its own strengths, enabling the labeling of drugs and ligands in native form without altering their pharmacological properties; its short half-life (~20 min) allows multiple same-day scans with low radiation burden, and advances in radiochemistry now permit incorporation into diverse functional groups—though its use remains limited by the need for on-site cyclotron production and rapid synthesis. ^{11}C-radioligands are particularly impactful in neurology and cardiology, where they provide unique tools for studying neurotransmitter systems, protein aggregates, and brain metabolism, as well as myocardial metabolism and innervation [6]. Other positron-emitters are commonly used for their peculiar characteristics in PET imaging, as listed in Table 1. Among them, nitrogen-13 (^{13}N, half-life $t_{1/2}$ = 10 min) and oxygen-15 (^{15}O, half-life $t_{1/2}$ = 2 min) are short-lived PET radionuclides, thus making them unsuitable for multiple-step radiosynthesis in most scenarios. However, they find clinical application in perfusion and metabolic studies, where rapid tracer kinetics are advantageous.

In addition to organic radionuclides, radiometals broaden the scope of PET by enabling the labeling of complex biological vectors, including peptides, proteins, and antibodies. Notable examples are gallium-68 (^{68}Ga, $t_{1/2}$ = 67.7 min), copper-64 (^{64}Cu, $t_{1/2}$ = 12.7 h), and zirconium-89 (^{89}Zr, $t_{1/2}$ = 78.4 h). Their incorporation relies on coordination chemistry, in which the radiometal is complexed with a suitable chelator that is subsequently conjugated to the targeting vector. The generally mild labeling conditions and the broad range of available half-lives—from a few hours to several days—allow selection of the most appropriate radionuclide according to the intended clinical or research application [7]. Notably, radiometals and longer-lived radionuclides provide an ideal framework for theranostic applications, relying on matched pairs of agents to enable both diagnosis and treatment of tumors on the same biological and molecular basis. To do so, radionuclides with different properties are attached to similar—or ideally identical—scaffolds, which can bind the target of interest with high affinity and thereby exert either diagnostic or therapeutic activity. Unlike diagnostic isotopes, which primarily decay through β^+ or γ-emission, therapeutic radionuclides act by releasing cytotoxic radiation characterized either by a very high energy but an extremely short tissue range (α particles, Auger electrons), or by moderately energetic β^- emissions with longer

 doi:10.20944/preprints202604.0617.v1

penetration in tissues. Such radiation is theoretically capable of directly damaging the DNA of cancer cells, thereby impairing their ability to replicate and inducing apoptosis.

The cornerstone of the modern theranostics is lutetium-177 (^{177}Lu), a therapeutic β^--emitting radionuclide with a tissue penetration of 1–2 mm, making it suitable for targeting small tumors or micrometastases while limiting damage to surrounding tissues. In addition, it emits low energy γ radiation, which is useful for imaging and dosimetry during therapy. Clinically, ^{177}Lu has been successfully employed in the development of radiopharmaceuticals such as [^{177}Lu]Lu-DOTATATE (Lutathera®) for neuroendocrine tumors (NETs) and [^{177}Lu]Lu-PSMA-617 (Pluvicto®) for prostate cancer, which have set new standards in targeted radionuclide therapy. Both agents can form theranostic pairs: the vector (DOTATATE) can be labeled with a PET radionuclide (^{68}Ga or ^{64}Cu) to identify patients with somatostatin receptor–positive tumors prior to therapy with Lutathera®. Similarly, PET imaging with [^{68}Ga]Ga-PSMA-11 (or [^{18}F]-labeled PSMA ligands) allows the selection of prostate cancer patients eligible for treatment with Pluvicto®. Other emerging theranostic combinations are ^{124}I/^{131}I for thyroid cancer and ^{86}Y/^{90}Y for dosimetry and therapy [8].

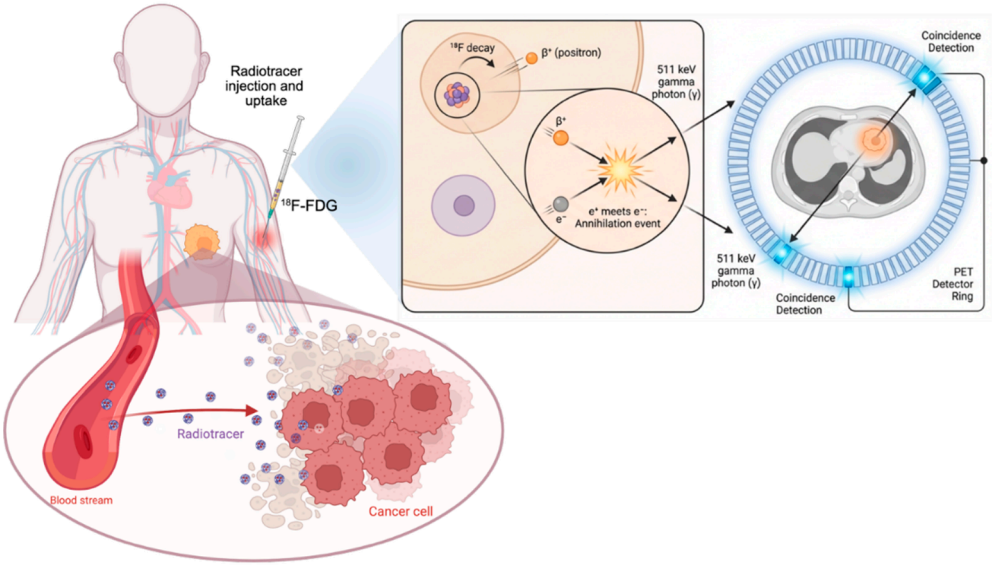

Figure 1. Schematic representation of the physical principles underlying positron emission tomography (PET). *(i) Radiotracer injection and uptake*: As an example, ^{18}F-FDG is injected and accumulates in metabolically active tissues such as tumors. *(ii) Positron emission:* The ^{18}F nucleus incorporated in the radiotracer undergoes β^+ decay, emitting a positron (β^+). The latter travels a short distance through the surrounding tissue while losing kinetic energy. *(iii) Annihilation event:* The positron (e^+) encounters an electron (e^-), resulting in mutual annihilation and conversion of their mass into two 511-keV γ photons emitted ~180° apart. *(iv) Coincidence detection and image reconstruction:* These coincident photons are detected by opposing scintillation detectors in the PET scanner, enabling reconstruction of the line of response and, through computational algorithms, the three-dimensional distribution of the radiotracer *in vivo*. .

Table 1. Overview of commonly employed positron-emitting isotopes.

Isotope	Half-life	Mode of decay	Main application area	Clinical examples of PET pharmaceuticals

 doi:10.20944/preprints202604.0617.v1

^{18}F	109.8 min	β+ (97%), EC (3%)	Oncology Neurology	[^{18}F]FDG – reference tracer; gold standard in oncology (solid tumors, lymphomas); also used in infection/inflammation [9]. [^{18}F]FLT – investigational tracer for cellular proliferation and early therapy response [10]. [^{18}F]FET – widely used for brain tumors (gliomas) [11]. [^{18}F]NaF – bone imaging [12], and vascular disorders [13]. [^{18}F]PSMA and [^{18}F]fluciclovine – prostate cancer [14]. [^{18}F]fluoroestradiol – estrogen receptor (ER)-positive breast cancer [15]. [^{18}F]FDOPA –dopaminergic nerve terminals in the striatum of patients with suspected Parkinsonian syndrome [16]. [^{18}F]flortaucipir –aggregated tau neurofibrillary tangles in Alzheimer's disease [17].
^{11}C	20.4 min	β+ (100%)	Neurology Cardiology	[^{11}C]raclopride - striatal dopamine binding in autism spectrum disorder [18]. [^{11}C]PIB - β-amyloid deposits in Alzheimer's disease [19]. [^{11}C]acetate – measures oxidative metabolism and myocardial perfusion; also applied in oncology (e.g., bladder carcinoma, brain tumors) [20].
^{13}N	10 min	β+ (100%)	Cardiology	[^{13}N]NH_3 – myocardial perfusion imaging (rest/stress) for ischemic heart disease [21].
^{15}O	2 min	β+ (100%)	Cardiology & Neurology (perfusion studies)	[^{15}O]H_2O - gold standard tracer for quantitative myocardial and cerebral perfusion imaging [22].
^{124}I	4.2 d	β+ (23%), EC (77%)	Oncology	[^{124}I]NaI – PET surrogate for ^{131}I therapy, used for thyroid imaging, diagnosis, and dosimetry in

 doi:10.20944/preprints202604.0617.v1

				differentiated thyroid cancer and hyperthyroidism [23,24].
^{44}Sc	4.0 h	β+ (94%), EC (6%)	Oncology	[^{44}Sc]ScDOTATOC/-TATE - NETs [25]. [^{44}Sc]ScPSMA-617 – prostate carcinoma [26].
^{64}Cu	12.7 h	β+ (17%), EC (44%), β- (39%)	Oncology	[^{64}Cu]CuDOTATATE - NETs [27]. [^{64}Cu]CuPSMA-617– prostate carcinoma [28].
^{68}Ga	67.7 min	β+ (89%), EC (11%)	Oncology	[^{68}Ga]GaDOTA-TATE/-TOC/-NOC - NETs [29]. [^{68}Ga]GaPSMA-11- prostate cancer [30].
^{82}Rb	1.3 min	β+ (95%), EC (5%)	Cardiology	[^{82}Rb]RbCl – myocardial perfusion imaging [31].
^{86}Y	14.7 h	β+ (32%), EC (68%)	Oncology	[^{86}Y]Y-DOTA-Phe^{1}-Tyr^{3}-Octreotide – PET surrogate for ^{90}Y therapy, enabling dosimetry and biodistribution assessment in NETs [32].
^{89}Zr	78.4 h	β+ (23%), EC (77%)	Oncology	[^{89}Zr]trastuzumab - HER2-positive breast cancer [33]. [^{89}Zr]Zr-DFO-onartuzumab - PET surrogate for predicting response to Met-targeted radioligand therapy in pancreatic cancer [34].

PET has proven to be an exceptionally powerful technique for diagnosing and monitoring the progression of diseases such as neurological disorders, cancer, cardiovascular disorders, and infections [35]. Moreover, its use contributes to guide therapeutic interventions, such as radiotherapy, drug administration and surgery, by monitoring the effectiveness of these treatments. Beyond its diagnostic applications, PET is crucial in drug research and development, offering rapid *in vivo* data access. In pre-clinical phases, it helps determine whether a biological target is associated with a specific disease, evaluates the biological parameters of drug candidates—such as target engagement, nonspecific binding, blood-brain barrier (BBB) penetration, and metabolism—to assess their suitability for treating a given condition, and provides valuable insights into the drug's mechanism of action. In clinical trials, PET aids to establish dose ranges with small volunteer groups, thus accelerating drug development, reducing adverse effects, and minimizing trial sizes [36].

Based on all these considerations, it is reasonable to assume that a radiotracer must meet certain key requirements to be effective. These include high specificity and selectivity for the target, rapid plasma clearance, and low plasma protein binding, as well as neutral and hydrophilic properties to enhance elimination and minimize the effective radiation dose. Additionally, the radiotracer must exhibit low toxicity, good *in vivo* stability, and sub-nanomolar or nanomolar affinity for the physiological target to avoid interfering with normal biological functions. It should also be easy and

 doi:10.20944/preprints202604.0617.v1

quick to produce, with a reasonable radiochemical yield, and be readily detectable during analysis. Reproducible pharmacokinetics and limited or measurable metabolism are essential, along with a half-life that aligns with the biological process being studied. Finally, the radiotracer must undergo β^+ decay, as other types of emission are not suitable for PET imaging and would result in unnecessary radiation exposure for the patient.

Thus, the success of PET technology largely depends on the development of safe, highly sensitive and specific radiotracers targeting clinically relevant biomarkers. These include the G protein-coupled receptor (GPCR) superfamily that comprises over 800 proteins encoded by the human genome, thus representing the largest and most ubiquitous family of transmembrane receptors that reside on cell surfaces [37]. These receptors function as highly adaptable membrane sensors, effectively serving as "message inboxes." They can detect a wide range of physicochemical stimuli, including ions, small organic molecules (such as odorants, vitamins, and neurotransmitters), photons, hormones, growth factors, lipids (like sterols and fatty acids), peptides, and proteins (including glycoproteins and chemokines). By doing so, they translate extracellular signals into intracellular responses across the plasma membrane. When GPCRs are activated intracellularly by the binding of a specific signaling molecule or "agonist", they trigger a cascade of signals mediated by heterotrimeric G proteins (G_s, $G_{i/o}$, $G_{q/11}$, and $G_{12/13}$), arrestins, and various downstream effectors [38]. G proteins control the activity of enzymes and channels, leading to changes in the levels of second messengers within cells and, consequently, influencing their functional activities. These processes operate through pathways involving protein kinases, modifications in the phosphorylation or activity of proteins, ion channel regulation, low molecular weight GTP-binding proteins, and shifts in gene expression. By employing these diverse signaling mechanisms, GPCRs govern a broad spectrum of cellular functions, ranging from fundamental aspects of cell biology—such as metabolism, growth, apoptosis, and migration—to specialized cellular responses, including muscle contraction or relaxation, glandular and epithelial secretion, and modifications in neuronal activity.

Consequently, GPCR signaling is pivotal in various pathological processes, including the regulation of the immune system, inflammatory responses, mood and behavior modulation, and the maintenance of homeostasis. This makes GPCRs the major pharmacological target, with approximately 35% (~700) of all drugs approved by the US Food and Drug Administration (FDA) targeting this receptor family [39]. Extensive analyses of all clinical trial candidates mapped onto the GPCR superfamily tree identified roughly 321 agents, 20% of which target 66 potentially novel GPCRs with no approved drugs to date [37].

For the longest time, drugs targeting GPCRs have generally been developed without the support of high-resolution structural knowledge, which indeed are immensely valuable for providing a wide range of templates for a rational drug design [40]. Furthermore, recent landmarks in cryo-electron microscopy (cryo-EM), which led to the characterization of more than 500 molecular structures, have given a strong impetus to improve our understanding of GPCR structural biology [41].

The long track record of progress in the structural biology and pharmacology of GPCRs, along with rapid advances in computational techniques, has been the keystone of the success in the GPCR research area in the past few decades. This progress has also significantly contributed to enriching the radiopharmaceutical landscape, highlighting the huge potential of GPCRs as molecular targets for non-invasive PET imaging across a wide range of diseases. In fact, as biomarkers, GPCRs can be studied on circulating cells, such as tumor or fetal cells, within exosomes found in blood or urine, or as cell surface proteins detectable through specialized probes. These methods have the potential to enhance personalized and precision medicine approaches for GPCR-based therapies by identifying individuals or patient groups expressing specific GPCRs that can be targeted with appropriate therapeutic agents, with treatment responses monitored through biomarker analysis [42].

This review highlights the potential of GPCRs as molecular targets for non-invasive imaging via PET, as they are central to numerous physiological processes and are involved in a wide range of diseases. We selected the most innovative patents from 2020 to 2025 that paved the way to radiolabeled GPCR probes, enabling the visualization and quantification of these receptors *in vivo*,

 doi:10.20944/preprints202604.0617.v1

and significantly improving our understanding of their role in health and disease. We classified the patented radiotracers according to their diagnostic applications, grouping them by target pathology. Recurrent structural motifs across the analyzed compounds are highlighted and discussed alongside their biological data.

2. Landmark Patents (2020–2025): Classification by Disease Area and GPCR Biomarker

2.1. Oncology

GPCRs are now being used as promising biomarkers in oncology, aiding in early diagnosis, staging and restaging, monitoring treatment response, and radiotherapy planning.

While the question of whether GPCR and G protein mutations may drive cancer progression remains debated [43], GPCR activity and post-receptor signaling events greatly contribute to the control of key cellular processes associated with the hallmarks of cancer, such as proliferation, metabolism, programmed cell death, ion and nutrient transport, and migratory behavior [44]. Moreover, substantial evidence supports aberrant GPCR expression across various cancer types. For instance, tumors of the neuroendocrine system frequently display a high prevalence of the serotonin 5-HT_4 receptor, the glucagon-like peptide-1 (GLP-1) receptor, and the melanocortin-2 receptor (MC2R), whereas lysophosphatidic acid receptor 5 (LPA_5) and the chemokine CCR6 receptor are predominantly expressed in pancreatic ductal adenocarcinoma. Beyond tumor cells, GPCRs are also expressed by multiple cell types within the tumor microenvironment, including stromal (fibroblast), vascular, immune, and inflammatory cells.

In this context, a study employing an unbiased (GPCRomic) approach systematically identified and quantified GPCR expression across multiple cancer cell types, revealing an unexpectedly broad and heterogeneous GPCR landscape. Notably, in each tumor type a common core set of GPCRs was identified, with several cancer cell types displaying expression of more than 150 distinct receptors, including those subsets detected at relatively high levels. These findings support the concept of tumor-specific "GPCR signatures," whereby individual GPCRs or defined receptor patterns may serve as novel diagnostic biomarkers and/or therapeutic targets [45].

Although further validation is needed to understand how GPCRs may contribute to the malignant phenotype and may represent therapeutic targets, this comprehensive profiling underscores the extraordinary potential of GPCR expression patterns as a rich and still largely untapped source for PET imaging in oncology.

2.1.1. Somatostatin Receptors (SSTRs)

Somatostatin (also known as growth hormone-inhibiting hormone, GHIH), is an endogenous peptide that exerts inhibitory effects on virtually all endocrine and exocrine secretions. It is produced by pancreatic δ-cells and inhibits the release of insulin and glucagon; furthermore, it is generated in the hypothalamus, to inhibit the release of growth hormone (GH), adrenocorticotropic hormone (ACTH), prolactin and thyroid-stimulating hormones (TSH) from the anterior pituitary. Somatostatin derives from the 116-amino acid precursor preprosomatostatin, which undergoes proteolytic cleavage to prosomastatin that is further processed into two active isoforms: somatostatin-14 (SST-14) and somatostatin-28 (SST-28). Their effects are mediated by five GPCRs (SSTR1–5), which show distinct tissue distributions [46,47]. SSTR1 is abundant in the jejunum and stomach; SSTR2 in cerebrum, pituitary, pancreas, intestines and kidney; SSTR3 in the brain and testis; SSTR4 in fetal and adult brain and lungs; and SSTR5 in the brain, pituitary gland, pancreatic α- and γ-cells as well as in the gastrointestinal tract. Importantly, SSTRs are overexpressed in several tumors and endocrine disorders, such as acromegaly, making them key targets for diagnostic imaging.

In 1994, the first peptide-based radiopharmaceutical, ^{111}In-pentetreotide, was approved by the FDA under the name Octreoscan® for the diagnosis of NETs and certain non-NETs expressing SSTRs. In this compound, the selective SSTR2 agonist octreotide is conjugated to indium-111 through the

 doi:10.20944/preprints202604.0617.v1

chelator diethylenetriaminepentaacetic acid (DTPA) [48]. In the following years, DOTA-chelated peptides labeled with radioactive metals became available for PET imaging applications [49]. More recently, ^{68}Ga-DOTA-conjugated peptides, such as [^{68}Ga-DOTA^{0}-Tyr^{3}]octreotide, (^{68}Ga-DOTA-TOC, ^{68}Ga-edotreotide), [^{68}Ga-DOTA^{0}-1NaI^{3}]octreotide (^{68}Ga-DOTA-NOC) and [^{68}Ga-DOTA^{0}-Tyr^{3}]octreotate (^{68}Ga-DOTA-TATE), have led to significant improvements in PET imaging. These agents provide superior spatial resolution and more favorable pharmacokinetics compared to conventional SSTR scintigraphy, although most of them are not fully selective for a specific SSTR subtype.

The search for optimized SSTR2-targeting ligands remains highly relevant. In 2024, a patent application by Crinetics Pharmaceuticals, Inc. proposed a new platform of small molecule drug conjugates (SMDCs) for selective cancer therapeutics or diagnostics [50]. These non-peptide SST2R ligands, built on a 4-piperidinyl-3-benzimidazole-6-arylpyridine scaffold (general formula, Figure 2), can be conjugated via spacer and/or linker moieties to suitable drug cargos or payloads, including not only chemotherapeutic agents but also radionuclides, thereby opening opportunities for PET imaging and theranostic applications. The central concept is to deliver functional agents that, on their own, exhibit limited selectivity, but which, when conjugated to an SSTR2 ligand, can be selectively directed to cancer cells, thus enhancing their therapeutic window.

To assess the biological activity of the SMDCs of the present invention, the compounds were first evaluated in CHO-K1 cells expressing SSTR2, where they consistently reduced intracellular cAMP levels in line with an agonistic profile. Internalization assays highlighted the impact of linker selection on receptor-mediated uptake, while antiproliferative effects were evaluated in NCI-H524 small cell lung cancer cells. However, subsequent *in vivo* investigations focused primarily on the indium-111 (^{111}In)–radiolabeled form of Compound 1 (Figure 2), consisting of the cytotoxic payload monomethyl auristatin E (orange), a linker moiety (pink), and the SSTR2-targeting ligand (blue). The biodistribution of [^{111}In] Compound 1 was evaluated in female Swiss nude mice bearing xenografts of the SSTR2-positive rat pancreatic tumor cell line AR42J, showing high and sustained tumor uptake in a receptor-specific manner, with competition studies confirming selectivity. Non-specific uptake was limited to the kidneys, consistent with renal excretion as the main elimination pathway.

While the document refers to potential PET applications of the SMDCs, it does not provide experimental validation to support this aspect.

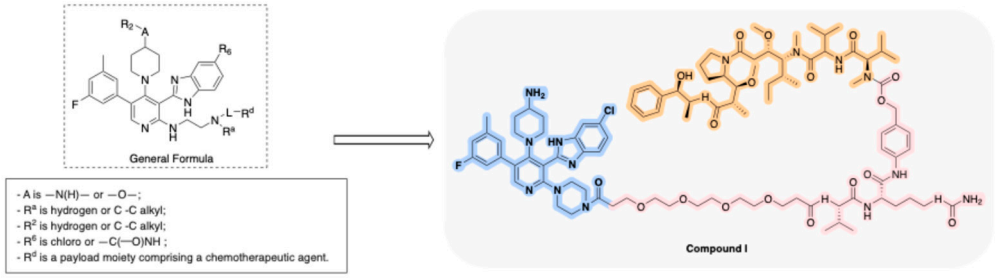

Figure 2. General formula of the non-peptide SSTR2 ligands based on a 4-piperidinyl-3-benzimidazole-6-arylpyridine scaffold (left) and representative structure of Compound 1 (right), comprising the SSTR2-targeting moiety (blue), linker (pink), and cytotoxic payload monomethyl auristatin E (orange) [50].

In recent years, the scientific community has increasingly focused on other SSTR subtypes expressed in certain tumors, with selective SSTR3-targeting ligands emerging as promising derivatives. SSTR3 is overexpressed in several malignancies, including gastroenteropancreatic neuroendocrine tumors (GEP-NETs), pituitary adenomas, and various hematological cancers such as sarcomas, myelomas, lymphomas, and leukemias. Moreover, SSTR3 expression has been reported in a wide range of solid tumors, including those of the pancreas, colon, breast, prostate, ovary, liver, kidneys, and lungs. Notably, SSTR3 is the only somatostatin receptor associated with p53-mediated apoptosis and cell cycle arrest, and it displays significantly higher internalization rates compared to

 doi:10.20944/preprints202604.0617.v1

other subtypes. These distinctive features, combined with its widespread expression in tumors, make SSTR3 a highly promising target for both diagnostic and therapeutic applications in oncology [51].

Accordingly, the May 2024 patent by Starget Pharma Ltd. specifically focuses on this receptor subtype, reporting a novel class of 28 conformationally constrained somatostatin analogs with high affinity and selectivity for SSTR3 [52]. The general structure of these compounds (R^1–R^2–D-Phe–R^3–Cys–R^4–D-Trp–Lys–Thr–R^6–R^5) consists of a sequence of amino acids interspersed with various R groups, strategically arranged to enhance receptor binding, subtype selectivity, and pharmacokinetic performance (general formula, Figure 3). A disulfide bridge between the cysteine residue and R^5 group, consisting of an *N*-thioalkyl-glycine (NTAG), confers conformational rigidity and improved metabolic stability. The scaffold also supports *N*- or *C*-terminal conjugation with functional moieties such as radiometal chelators (e.g., DOTA), linkers, or bioactive agents, providing a versatile platform for the development of somatostatin analogs for both diagnostic and therapeutic purposes.

Among the tested compounds, SEQ ID NO: 4 (Figure 3) fully exemplified this dual potential, proving to be a nanomolar ligand with high selectivity for human SSTR3 and significantly lower affinity for the other SSTR subtypes. An additional set of pharmacological assays evaluated its potential off-target interactions, revealing no detectable agonistic or antagonistic activity across a panel of 167 human GPCRs. Furthermore, successful radiolabeling with ^{68}Ga confirmed its suitability for PET imaging applications. Altogether, these findings highlight the superiority of this compound in fulfilling the key requirements for an SSTR3-selective radioligand. SEQ ID NO: 4 also demonstrated therapeutic relevance, supporting its classification as a theranostic candidate. Comparative studies in *h*SSTR3-transfected CHO cells showed that SEQ ID NO: 4 induces strong β-arrestin–mediated receptor internalization. Although it shares an EC_{50} comparable to the native hormone SRIF-14, SEQ ID NO: 4 elicited a β-arrestin response twice as strong, identifying it as a novel (first time known) superagonist of *h*SSTR3.

In vivo PET-CT imaging was performed following intravenous injection of SEQ ID NO: 4, with dynamic scans acquired for up to 240 minutes in mice and 270 minutes in rats. Biodistribution analysis revealed substantial tumor uptake in both models, with a favorable tumor-to-kidney ratio of approximately 50% observed in rats.

To further assess translational potential, a first-in-human PET-CT scan was conducted in a 37-year-old male patient with Desmoplastic Small Round Cell Tumor (DSRCT) known to express SSTR3. Imaging was performed at 30- and 120-minutes post-injection (~600 MBq). The tracer showed rapid blood clearance and renal excretion, along with clear and specific tumor uptake. The PET signal was consistent with SSTR3 expression and aligned with the patient's clinical prognosis. Importantly, the biodistribution confirmed the compound's high selectivity for SSTR3, with no uptake in off-target organs and no evidence of unexpected toxicity, supporting both its diagnostic value and safety profile.

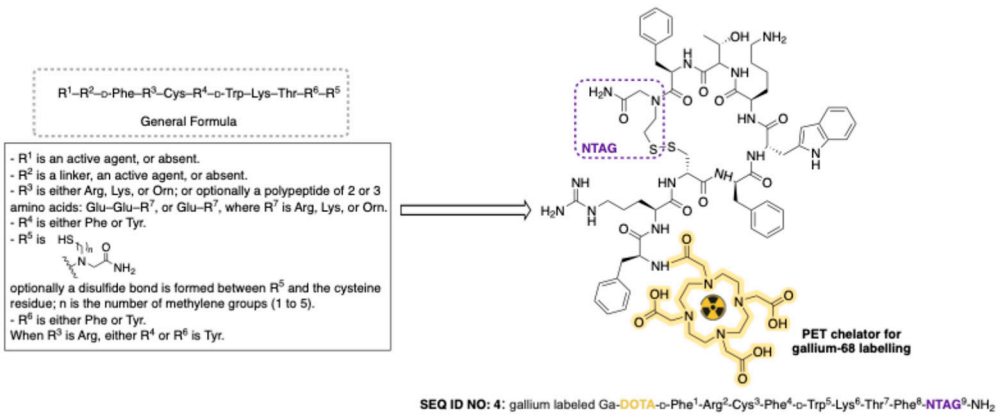

 doi:10.20944/preprints202604.0617.v1

Figure 3. General structure of the conformationally constrained somatostatin analogs targeting SSTR3 (left) and representative structure of SEQ ID NO: 4 (right), illustrating the cyclic peptide scaffold with the characteristic NTAG moiety (purple) and its conjugation with a DOTA chelator for radiometal labeling (yellow) [52].

2.1.2. Cholecystokinin 2 Receptor (CCK2R)

The cholecystokinin 2 receptor (CCK2R, also known as cholecystokinin B receptor or CCKBR), a member of the GPCR family, has emerged as an attractive molecular target for both imaging and therapy in oncology, owing to its overexpression in several malignancies, including medullary thyroid cancer (MTC), small-cell lung cancer (SCLC), gastrointestinal stromal tumors (GIST), gliomas, as well as colorectal (CRC), breast (BC), and ovarian cancers. CCK2R is physiologically activated by gastrin, an endogenous linear peptide hormone initially encoded as pre-progastrin. Following post-translational enzymatic cleavage, progastrin is processed by G cells of the duodenum and pyloric antrum into mature gastrin, which is secreted into the bloodstream. In humans, gastrin occurs in different molecular forms, primarily big-gastrin (G-34), little-gastrin (G-17), and mini-gastrin. These peptides share a conserved C-terminal amino acid motif that enables high-affinity binding to CCK2R. On this basis, several studies have investigated radiolabeled gastrin analogues for molecular imaging and peptide receptor radionuclide therapy (PRRT), including the mini-gastrin derivative PP-F11N (DOTA-(D-Glu)$_6$-Ala-Tyr-Gly-Trp-Nle-Asp-Phe-NH_2), where the DOTA chelator stably coordinates radionuclides such as ^{177}Lu (therapy) and ^{68}Ga (PET imaging) (Figure 4) [53].

It is well established that high and sustained tumor uptake of a radiopharmaceutical directly depends on the expression level of its molecular target. This is particularly relevant for CCK2R, where, in some indications, receptor prevalence in tumor tissues has been reported to be low, with only 10–20% of patients exhibiting sufficient expression levels to enable effective PRRT. Moreover, the assessment of CCK2R expression by standard techniques, such as immunohistochemistry (IHC) or autoradiography, remains challenging, likely due to the limited selectivity and specificity of available anti-CCK2R antibodies.

To address this limitation, the Paul Scherrer Institute patented a biomarker-driven strategy demonstrating a strong correlation between CCKBR mRNA levels, receptor protein abundance, and radioligand uptake [54]. On this basis, CCKBR mRNA was proposed as a robust predictive biomarker for patient stratification in therapeutic or imaging procedures involving radiolabeled gastrin analogues targeting CCK2R.

Importantly, this patent does not introduce a novel targeting vector but builds upon the previously claimed mini-gastrin derivative PP-F11N [55], which had already demonstrated favorable properties, including high stability, suitable biodistribution, and reduced renal uptake when labeled with ^{177}Lu.

Moreover, the patent published in August 2023 [56] discloses ^{68}Ga-PP-F11N (Figure 4) as a specific PET imaging agent for CCKBR-positive tumors and reports a biodistribution profile closely resembling that of ^{177}Lu-PP-F11N, thereby supporting its use in pre-selecting patients likely to benefit from CCK2R-targeted radionuclide therapy. Thus, in US2024401145A1, PP-F11N was investigated as a case study to illustrate a biomarker-guided clinical workflow integrating CCKBR mRNA quantification in tumor biopsies to identify CCK2R–positive cases, PET-based confirmation of receptor expression using ^{68}Ga-PP-F11N, and subsequent therapy with ^{177}Lu-PP-F11N (Figure 4) in selected patients, with ^{111}In-PP-F11N reserved for preclinical dosimetry. This integrated approach provides quantitative cut-off values for clinical decision-making and underscores the translational relevance of mRNA-based patient selection for CCK2R–targeted PET imaging and PRRT, while consolidating PP-F11N as a clinical reference ligand [54].

 doi:10.20944/preprints202604.0617.v1

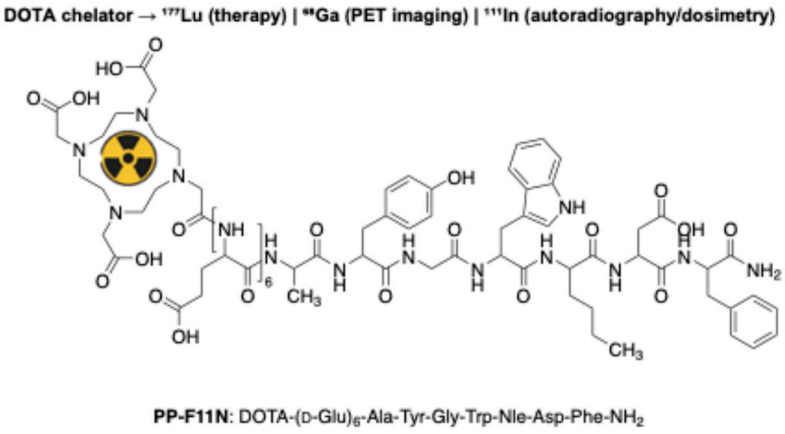

Figure 4. Structure of PP-F11N and its conjugation to a DOTA chelator enabling radiolabeling with different radionuclides (^{177}Lu, ^{68}Ga, ^{111}In), each evaluated for distinct diagnostic or therapeutic applications [53–56].

2.1.3. Dual-Receptor Targeting Strategy: SSTR2 and CCK2R

SSTRs can be co-expressed with other targets in heterogeneous tumors. For instance, aggressive NETs frequently express both SSTR2 and CCK2R. A ligand capable of engaging both receptors may improve imaging sensitivity and therapeutic efficacy compared to agents targeting a single receptor. Moreover, a modular design may support broader tumor uptake—addressing SSTR2-positive, CCK2R-positive, or double-positive cells—and promote enhanced retention of the radiopharmaceutical through multivalent binding mechanisms.

Dual-targeted radiopharmaceuticals addressing both SSTR2 and CCK2R represent the core concept of a patent dated 2024 [57]. These novel hybrid compounds hold promise for PET imaging of SSTR2- and CCK2R-positive tumors as well as for targeted radionuclide therapy of receptor-expressing lesions.

Figure 5 illustrates the modular design of a trifunctional molecule, where a trivalent branching unit (T) connects three domains: *(i)* a chelating group (E), *(ii)* a CCK2R-binding motif (Z_1), and *(iii)* an SSTR2-binding motif (Z_2), each joined by flexible spacers (L_1–L_3). The SSTR2-targeting unit is typically a somatostatin-derived peptide (e.g., octreotide or octreotate), while the CCK2R-binding domain is often derived from a modified cholecystokinin fragment. These pharmacophores are joined via a bifunctional linker, which frequently incorporates a metal-chelating group, such as DOTA or macrocyclic chelators, thereby enabling stable incorporation of diagnostic (such as ^{68}Ga or ^{111}In) or therapeutic (such as ^{177}Lu or ^{90}Y) radiometals. Variants of the linker (L_1–L_3), including polyethylene glycol (PEG) chains, neutral amino acid bridges (e.g., glycine or serine), or other bifunctional moieties, have been employed to modulate spatial arrangement and optimize dual receptor binding.

 doi:10.20944/preprints202604.0617.v1

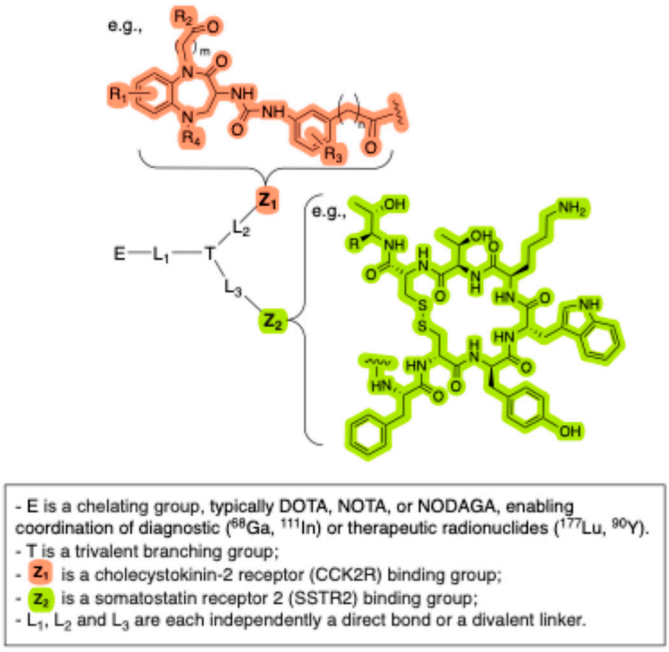

Figure 5. General formula of dual SSTR2- and CCK2R-targeting radioligands [57].

The patent further covers pharmaceutical formulations comprising any of the described compounds or their radiolabeled derivatives, in combination with pharmaceutically acceptable excipients. These formulations may include, for instance, sterile injectable solutions suitable for intravenous administration of the dual-target radiopharmaceutical. The scope also extends to kit formulations, such as lyophilized ligands intended to be combined with a radionuclide immediately prior to administration, and to methods of treatment or diagnosis involving the administration of any of the radiolabeled compounds described.

It should be noted, however, that while the patent outlines the potential use of these compounds in PET imaging, it does not present experimental evidence to support this application.

2.1.4. CXC Chemokine Receptor Type 4 (CXCR4)

CXCR4 is a GPCR expressed on monocytes, B cells, naïve T cells, neutrophils and eosinophils. It is involved in multiple physiological functions and interacts with its natural ligand chemokine ligand 12 (CXCL12), also known as stromal cell-derived factor 1 (SDF-1) [58]. Over the past decades, the CXCR4–CXCL12 signaling axis has been the focus of extensive research because of its key contribution to the onset and progression of several hard-to-treat conditions, including HIV infection, inflammatory disorders, and metastatic cancers such as breast, gastric, and non-small cell lung cancer [59]. This pathway promotes angiogenesis and mobilization of bone marrow–derived myeloid cells, facilitating tumor recurrence and metastasis and contributing to resistance against both conventional and targeted treatments. Approaches aimed at blocking CXCR4/CXCL12-mediated chemotaxis—using antibodies, peptide-based inhibitors, or small-molecule antagonists—have shown promise in enhancing white blood cell mobilization while reducing metastasis by preventing tumor cell migration and their homing to secondary organs. Given its central role in cancer biology, CXCR4 has emerged as a compelling target for the development of both diagnostic imaging tools and therapeutic interventions.

A wide range of CXCR4-targeted PET tracers has been developed over the past years. While preclinical studies have yielded highly promising candidates with strong CXCR4 affinity and excellent targeting properties, the number of compounds that have advanced into clinical testing remains limited, and their translation has been hampered by unfavorable pharmacokinetics and/or suboptimal tumor uptake [60]. Nevertheless, ongoing efforts in CXCR4-targeted PET probe design and clinical validation are expected to overcome these challenges. Reflecting this trend, a 2023 patent

 doi:10.20944/preprints202604.0617.v1

from the Istituto Nazionale Tumori IRCCS – Fondazione G. Pascale drew on the highly specific CXCR4 antagonist R54 [61] as a structural template [62]. R54 is a cyclic heptapeptide (Ac-Arg-Ala-[D-Cys-Arg-Nal(2′)-His-Pen]-COOH) stabilized by a D-Cys^{3}–Pen^{7} disulfide bridge. It exhibits high serum stability, nanomolar CXCR4 affinity (IC_{50} ≈ 1.5–20 nM depending on the assay), and potent antagonist activity [63]. Thus, the present invention relates to labeled R54 analogues designed as tracers for the selective targeting and imaging of human CXCR4-expressing cells, including those found in primary and secondary tumors, as well as in neoplastic and tumor-infiltrating immune cells. To this end, the *N*-terminus of R54 was modified by introducing 6-(4-(aminomethyl)benzamido)hexanoic acid (AMBHA) as a linker, while NOTA and DOTA were employed as chelators for radiometal labeling (Figure 6). AMBHA was selected to provide an appropriate linker length, maintaining distance between the metal chelator and the interaction site on the receptor. The resulting conjugates, NOTA-AMBHA-R54 and DOTA-AMBHA-R54, were radiolabeled with ^{68}Ga and evaluated by *in vitro* and *in vivo* studies, which confirmed their potential for high-contrast CXCR4-targeted PET imaging. PET imaging and biodistribution studies were performed in athymic mice bearing CHO-*h*CXCR4 xenografts, with receptor expression confirmed by immunohistochemistry. Both [^{68}Ga]DOTA-AMBHA-R54 and [^{68}Ga]NOTA-AMBHA-R54 exhibited rapid clearance and negligible retention in non-target tissues, except for renal uptake. Consistent with its higher CXCR4 affinity, [^{68}Ga]NOTA-AMBHA-R54 demonstrated superior tumor accumulation and higher tumor-to-background ratios than the DOTA analogue. Competition with excess unlabeled R54 reduced uptake to background levels, confirming the specificity of the binding. PET imaging confirmed efficient targeting of CXCR4-positive tumors by both tracers and further highlighted the advantage of the NOTA derivative, with SUV_{max} values exceeding expectations from biodistribution data, and tracer uptake strongly correlated with CXCR4 expression levels. Overall, both [^{68}Ga]NOTA-AMBHA-R54 and [^{68}Ga]DOTA-AMBHA-R54 proved suitable as CXCR4-targeted PET tracers, with the NOTA analogue offering clear advantages in terms of affinity, tumor uptake, clearance, and imaging contrast. Its favorable pharmacokinetic profile also supports its potential as a scaffold for future therapeutic applications.

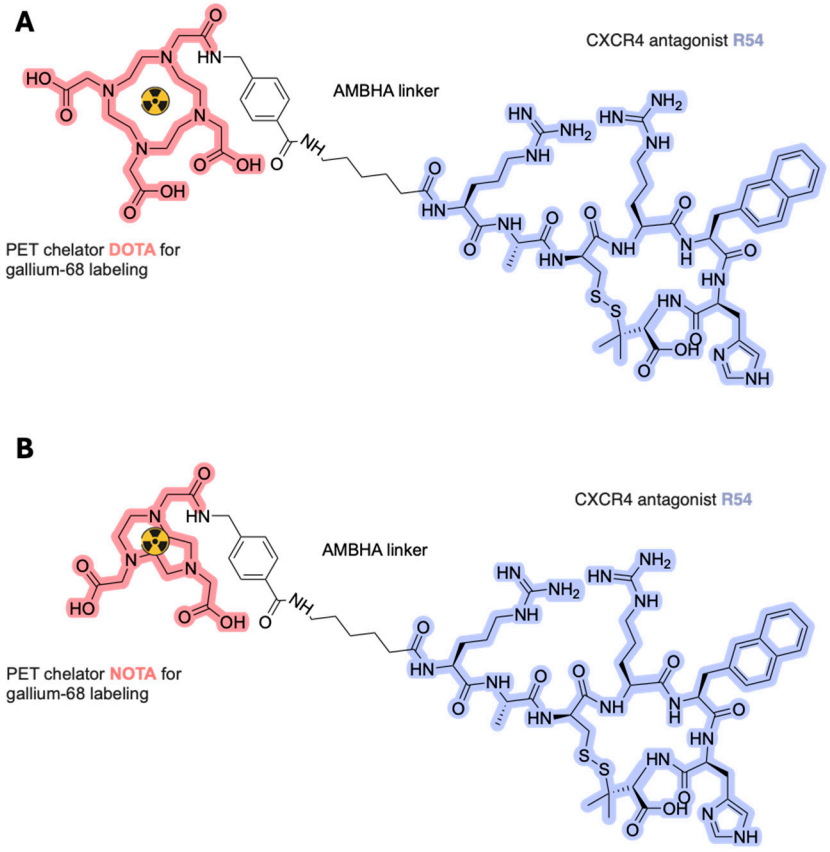

Figure 6. Structures of [^{68} Ga]DOTA-AMBHA-R54 (Panel A) and [^{68} Ga]NOTA-AMBHA-R54 (Panel B) [62].

 doi:10.20944/preprints202604.0617.v1

2.1.5. Neurokinin 1 Receptor (NK1R)

The neurokinin 1 receptor (NK1R, also known as tachykinin 1 receptor) is a member of the tachykinin receptor subfamily of GPCRs and is widely expressed in both the central and peripheral nervous systems. Its principal endogenous ligand is substance P (SP), which regulates diverse physiological processes, including hematopoiesis, wound healing, microvascular permeability, neurogenic inflammation, leukocyte trafficking, and cell survival [64]. Importantly, NK1R expression is upregulated in multiple-cancer types, such as astrocytoma, melanoma, prostate cancer, glioma, retinoblastoma, leukemia, and tumors of the pancreas, larynx, colon, stomach, and breast. The SP/NK1R axis has been documented to contribute to tumor progression by promoting mitogenesis, angiogenesis, cell migration, and metastasis; accordingly, NK1R antagonists have been proposed as promising therapeutic agents in oncology. Among them, aprepitant (commercially known as EMEND or L-754,030) is particularly noteworthy. Approved for the treatment of chemotherapy-induced nausea and emesis, aprepitant has also shown antitumor properties, supporting its potential candidacy for future applications in prostate cancer therapy [65]. The structure of this small-molecule NK1R antagonist inspired several structure–activity relationship (SAR) programs aimed at improving its pharmacokinetic properties, which had hampered clinical development [66]. The derivative portfolio has also been expanded with novel aprepitant analogues functionalized with a DOTA chelator and radiolabeled with ^{68}Ga or ^{177}Lu, to further investigate their potential as radiopharmaceuticals. In line with the search for novel NK1R-targeting agents derived from small-molecule antagonists, a 2025 patent disclosed 54 newly substituted 2-phenylpiperidine derivatives (general formula shown in Figure 7), predominantly designed as radioiodinated analogues — mostly intended for therapeutic applications, except for ^{124}I which enables PET imaging — for the diagnosis, treatment, and/or prevention of cancer [67]. Within this chemical series, several analogues demonstrated low-nanomolar affinity for NK1R across different NK1R-positive cancer cell lines, including neuroblastoma, colorectal, and osteosarcoma models. Binding assays were consistently accompanied by competition tests, which confirmed receptor-mediated uptake and minimal non-specific binding, thereby supporting the selective accumulation of these compounds at target sites. Although development has so far been limited to binding and cellular studies without *in vivo* imaging evidence, these compounds bind NK1R specifically and competitively, reinforcing the value of this chemical platform for diagnostic and therapeutic development.

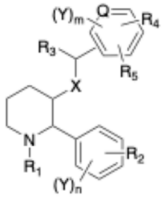

R^1 = H or $(CH_2)_p$Z with p=0,1,2,3
R^2 = H, OH, or F
R^3 = H or C_1–C_3 alkyl
R^4 = H, CF_3, O–C_1–C_6 alkyl, OCF_3, CN, F, or NO_2
R^5 = H, CF_3, O–C_1–C_6 alkyl, OCF_3, CN, F, or NO_2
Q = C or N
X = O or NH
Y = none or ^{127}I/^{123}I/^{124}I/^{125}I/^{131}I /^{211}At
Z = five- or six-membered heterocycle containing 1–3 nitrogen atoms and/or an N-oxide, optionally substituted with 0–3 groups independently selected from F, Cl, Br, I, OH, C_1–C_3 alkyl, oxo, or $(CH_2)_q$NH**R**$_6$ with q=2,3,4,5
R^6 = chelating moiety or radionuclide complex thereof

Figure 7. General formula of substituted 2-phenylpiperidine compounds [67].

2.1.6. Melanocortin Type 2 Receptor (MC2R)

 doi:10.20944/preprints202604.0617.v1

MC2R, the smallest human GPCR, is exclusively activated by adrenocorticotropic hormone (ACTH) and is predominantly expressed in the adrenal cortex. ACTH-mediated activation of MC2R initiates cAMP-dependent signaling pathways that promote glucocorticoid biosynthesis, primarily cortisol. Altered MC2R activity has been associated with impaired adrenal function, resulting in adrenal insufficiency, which may lead to hypoglycemia, abnormal stress responses, and metabolic imbalances [68]. Owing to its tissue-specific expression and its involvement in cortisol-producing adrenal tumors, MC2R represents an attractive molecular target for selective imaging and radionuclide-based therapeutic approaches in adrenal malignancies, including adrenocortical carcinoma (ACC). Zhao *et al.* reported a series of non-peptidic MC2R-targeting ligands based on a substituted aryl–heteroaryl scaffold, frequently functionalized with a piperidinyl moiety and a linker-separated chelating group or radionuclide complex (e.g., ^{111}In, ^{115}In, ^{67}Ga, ^{68}Ga, ^{177}Lu), including PET-relevant radiometals such as ^{68}Ga, although the platform is primarily proposed within a theranostic framework [69]. Biodistribution studies in non–tumor-bearing rats mainly focused on ^{111}In- and ^{177}Lu-labeled radiocomplexes of Compound 10 (Figure 8), revealing high and prolonged uptake in the adrenal glands. Receptor specificity was confirmed by selective blocking experiments, demonstrating MC2R-mediated uptake with minimal to no accumulation in non–MC2R-expressing organs. Subsequent imaging studies in MC2R-positive tumor models using ^{111}In–Compound 10 showed sustained and selective radiotracer accumulation in tumors as well as in adrenal glands, the only known site of endogenous MC2R expression. Specificity was confirmed by competition assays. Uptake in non-target organs, including blood, brain, and other tissues, was minimal, while renal and hepatic activity was transient and attributed to excretory pathways. Notably, ^{177}Lu-labeled derivatives demonstrated proof-of-concept antitumor efficacy in MC2R-expressing xenograft models, supporting the feasibility of MC2R-directed theranostic approaches.

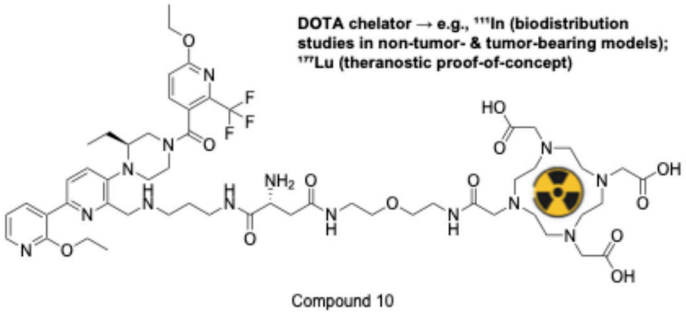

Figure 8. ^{111}In- and ^{177}Lu-labeled radiocomplexes of a representative non-peptidic MC2R-targeting ligand disclosed in the patent [69].

2.1.7. Kisspeptin Receptor (KISS1R)

KISS1R, also known as GPR54, is a member of the GPCR family and is overexpressed in several cancers, including breast cancer, renal cell carcinoma, and liver cancer. Its endogenous ligand, kisspeptin (KP), is a neuropeptide hormone that stimulates the hypothalamo–pituitary–gonadal (HPG) axis and is derived from proteolytic processing of a 145-amino-acid precursor encoded by the KISS1 gene. Kisspeptin is initially produced as a 54-amino-acid peptide and can be further processed into shorter biologically active fragments, among which kisspeptin-10 (KP10) shows high affinity for KISS1R. KP10 triggers $G_{q/11}$-mediated signaling, leading to phospholipase C activation and generation of inositol-1,4,5-triphosphate and diacylglycerol, which in turn induce intracellular calcium mobilization and MAPK pathway activation. This signaling cascade plays a key role in the modulation of the reproductive axis and endocrine function [70]. By regulating the release of gonadotropin-releasing hormone (GnRH) in the hypothalamus, this system drives pituitary gonadotropin secretion, which is essential for the onset of puberty and the maintenance of fertility [71].

 doi:10.20944/preprints202604.0617.v1

Beyond its reproductive role, the kisspeptin system exerts additional non-canonical functions in a range of pathological conditions, notably in cancer progression and metastasis. Altered KISS1/KISS1R signaling was found to be implicated in multiple tumor types, including melanoma, prostate and endometrial carcinomas, leiomyomas and leiomyosarcomas, breast cancer, choriocarcinoma, as well as epithelial and stromal ovarian tumors. Reduced receptor expression has been associated with increased tumor aggressiveness, invasion, and distant metastasis in gastric cancer, whereas in breast cancer KISS1R upregulation correlates with more aggressive disease and increased mortality risk [72,73]. Therefore, several kisspeptin peptide analogues have been developed to modulate kisspeptin signaling, effectively suppressing GnRH release and emerging as promising candidates for the treatment of hormone-dependent diseases, including prostate cancer. These analogues generally exhibit improved metabolic stability compared to native kisspeptins while retaining robust KISS1R agonist activity. In this context, the development of radiopharmaceuticals targeting KISS1R represents an attractive strategy for advancing cancer diagnosis and therapy [74]. For instance, Radionetics Oncology, Inc. has reported the development of a chemically versatile class of kisspeptin-derived conjugates described by the general Formula I (Figure 9). The disclosed conjugates feature extensive backbone and side-chain modifications, including non-natural amino acids, stereochemical inversions, and terminal functionalization. Importantly, this modular design enables conjugation to chelators or radionuclides, indicating a strategic focus on KISS1R-targeted diagnostic and therapeutic modalities [75]. This platform-based patent explicitly claims the use of KISS1R-targeted conjugates for PET imaging, outlining a versatile radiopharmaceutical strategy while leaving experimental PET validation to future studies.

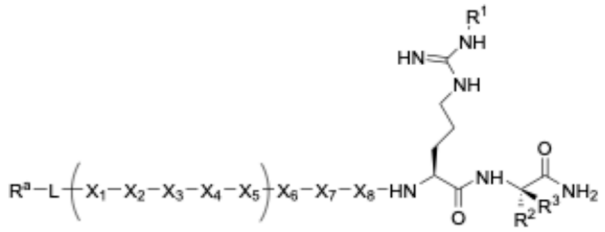

Formula (I)

X: optional amino acid residues
R^1 & R^3: H or C1–C4 alkyl.
R^2: aromatic or heteroaromatic moiety (e.g., substituted phenyl, pyridyl, indole, phenolic)
L: optional linker attached to any of X^1–X^5, or to X^6 when X^1–X^5 are absent.
R^a: chelating moiety or radionuclide complex thereof

Figure 9. Simplified schematic of the kisspeptin-derived conjugate platform defined by Formula (I) disclosed in WO2024206577 [75].

2.1.8. Neurotensin Receptor 1 (NTSR1)

Neurotensin (NT) is an endogenous tridecapeptide with the sequence *p*Glu–Leu–Tyr–Glu–Asn–Lys–Pro–Arg–Arg–Pro–Tyr–Ile–Leu, whose primary biological activity resides in the highly conserved *C*-terminal fragment NT (8–13). NT functions as a neurotransmitter in CNS, where it is involved in the regulation of pain modulation, thermoregulation, feeding behavior, reward, and also acts as a hormone in the gastrointestinal tract. Its biological effects are mediated by three neurotensin receptor (NTSR) subtypes: the classical GPCRs NTSR1 and NTSR2, and the non-GPCR receptor NTSR3 (sortilin) [76,77]. NTSR1 is the main mediator of NT signaling, displaying effects in both the CNS and the periphery, whereas NTSR2 is predominantly expressed in the brain and NTSR3 displays a broader tissue distribution. Although NT biology primarily originates in the CNS and, together with its receptors, constitutes the neurotensinergic system, marked NTSR1 overexpression has been reported in several solid tumors, including colorectal and pancreatic cancers—most notably pancreatic ductal adenocarcinoma (PDAC)—as well as breast, prostate, and both small- and non-

 doi:10.20944/preprints202604.0617.v1

small-cell lung cancers [78–80]. Accumulating evidence since the early 2000s has linked NTSR1 overexpression to disease progression, highlighting this receptor as an attractive target for oncological imaging and theranostic strategies [81]. Accordingly, high-affinity small-molecule NTSR1 antagonists, such as SR142948 (C-3, Figure 10), have enabled the development of NTSR1-targeted radioligands for tumor imaging and therapy, with preclinical validation and initial clinical evaluation in pancreatic cancer patients (e.g., ^{177}Lu-3BP-227 or C-2, Figure 10) [82,83]. However, prior derivatization strategies of SR142948 often resulted in reduced receptor binding affinity and compromised tumor-to-kidney and tumor-to-normal-organ ratios. These limitations have prompted the development of optimized SR142948 derivatives and next generation radioligands targeting neurotensin receptors to achieve a wider therapeutic window for clinical use. Along these lines, in August 2023, analogues of SR142948 and their novel radioligand derivatives, based on the general formula depicted in Figure 10, were developed, including compounds intended for PET imaging [84]. Competitive radioligand binding assays showed that all compounds display high affinity for NTSR1, with IC_{50} values in the 0.01–1 nM range, indicating that linker architecture between the aromatic core and the chelator can unexpectedly influence receptor binding. Functional activity was evaluated by FLIPR calcium-mobilization assays in HEK293 cells expressing human NTSR1, where several compounds inhibited neurotensin-induced intracellular Ca^{2+} signaling more effectively than the reference compound C-2.

The patent further reports comprehensive *in vivo* biodistribution studies of ^{177}Lu-labeled complexes in ASPC-1 pancreatic and HT-29 colorectal cancer xenograft models, revealing high and sustained tumor uptake, significantly improved tumor-to-normal organ ratios, and increased tumor AUC compared with the reference compound C-2, thereby highlighting the critical influence of linker design on the *in vivo* performance.

Importantly, PET imaging studies in ASPC-1 tumor-bearing mice using ^{68}Ga-labeled complexes demonstrated excellent tumor-to-normal tissue contrast over 180 minutes, with analogue I-6 emerging as the most promising candidate (Figure 10). These imaging data corroborated the biodistribution findings, thus supporting the use of these ligands for PET detection of NTR1-positive tumors.

Finally, the patent concludes with *in vivo* efficacy studies of ^{177}Lu- and ^{225}Ac-labeled complexes in ASPC-1 tumor-bearing mice, which demonstrated a pronounced tumor growth inhibition for selected compounds, further underscoring their therapeutic potential.

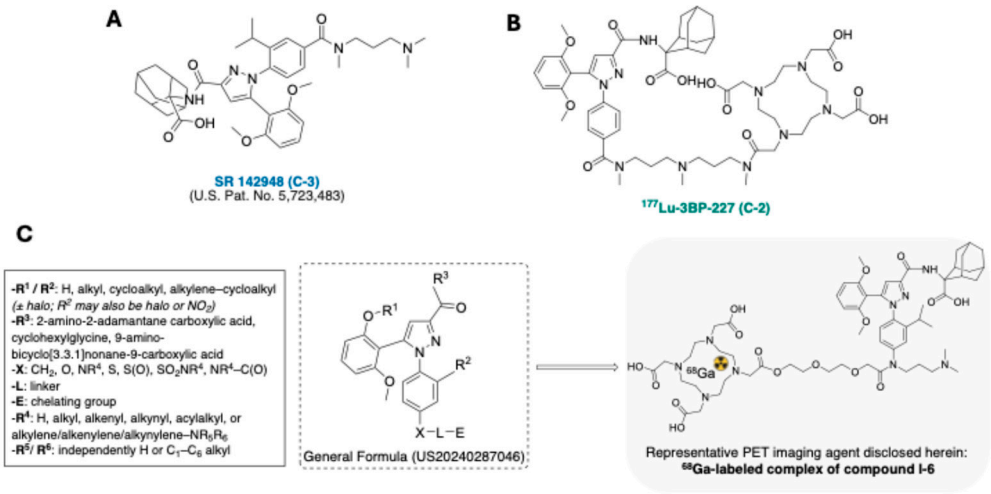

Figure 10. (A) Structure of SR142948 (C-3); **(B)** structure of ^{177}Lu-3BP-227 (C-2); **(C)** general formula of the newly developed SR142948-derived NTR1-targeting radioligands [84].

2.2. CNS Diseases

 doi:10.20944/preprints202604.0617.v1

Nowadays, PET scanning is a widely used imaging technique in the clinical neuroscience practice, as it greatly improves the understanding of the pathophysiology and treatment of central nervous system (CNS) diseases, such as neurodegenerative disorders, including Alzheimer's disease (AD), Parkinson's disease (PD) and multiple sclerosis, as well as psychiatric conditions, including schizophrenia and depression.

PET imaging effectively detects cerebral biomarkers using contrast agents composed of radioactive molecules rationally designed to selectively bind to target receptors, transporters, or to be metabolized by specific enzymes. By measuring the spatial distribution and concentration of these imaging agents within the CNS, PET enables a detailed quantitative analysis of biomarker dynamics, providing valuable insights into diverse CNS functions, among them neurotransmission, metabolic pathways, and inflammatory responses [85,86].

The ideal biomarker must have a high sensitivity and specificity, be easy to measure, provide reproducible results and reflect disease progression. Circulating microRNAs (miRNAs) and extracellular microvesicles - known as exosomes - are an example of molecular biomarkers that may be useful in the diagnosis of some pathological CNS conditions. Among others, it is worth noting tau protein, a cerebrospinal fluid biomarker considered a diagnostic criterion for AD. Accordingly, PET tau imaging agents are thought to represent the amount and distribution of tau protein plaques in the brain, providing insights into tau-related changes [87]. Additionally, one of the most widely studied biomarkers for PET imaging of neuroinflammation—which, as we know, is a significant hallmark of CNS disorders—is the 18 kDa translocator protein (TSPO), that is uniformly expressed on activated cells of the myeloid lineage, reactive astrocytes, and endothelial cells. However, TSPO PET tracers suffer from variable binding affinity in human subjects due to a polymorphism in the *TSPO* gene.

Several pieces of evidence strongly suggest that GPCRs are excellent biomarkers for PET imaging of CNS diseases [88]. One of the key strengths of GPCRs is their high specificity for certain cell types and physiological processes, allowing PET imaging to precisely target CNS signaling pathways while minimizing off-target effects. Unlike static biomarkers (e.g., protein aggregates), GPCRs provide dynamic functional insights by visualizing real-time processes such as neurotransmitter activity and receptor signaling. Notably, GPCR activity often changes at an early stage of disease progression, even before structural damage occurs, making them these receptors valuable for understanding disease onset and monitoring therapeutic responses.

Other advantages are the GPCR widespread expression across the CNS, enabling the study of various neurological conditions, and their well-characterized pharmacology as drug targets, that clearly facilitates the development of radiotracers.

2.2.1. Metabotropic glutamate receptors 2 and 3 (mGluR2 & mGluR3)

L-Glutamate is the major excitatory neurotransmitter in the CNS and plays a crucial role in regulating several neurological functions. It acts through two major receptor families: ionotropic glutamate receptors (iGluRs) and metabotropic glutamate receptors (mGluRs) [89,90]. mGluRs (mGluR1–mGluR8), members of the GPCR superfamily, are classified into three groups. Among them, group II receptors—mGluR2 and mGluR3—are primarily located on presynaptic nerve terminals where they exert a negative feedback loop to the release of glutamate into the synapse [91]. Therefore, group II ligands, whether acting orthosterically or allosterically, relieve the inhibitory control on glutamate release, thereby enhancing glutamatergic signaling. This mechanism makes them promising candidates for the treatment of neurological disorders associated with dysregulated glutamatergic transmission, such as psychosis, mood disorders, AD, and cognitive or memory impairments [92]. For instance, Roche has investigated the mGluR2/3 antagonist RO4995819 in clinical trials as an adjunctive therapy for Major Depressive Disorder unresponsive to standard antidepressants and has also disclosed mGluR2/3 negative allosteric modulators (NAMs) as potential treatments for autism spectrum disorders.

 doi:10.20944/preprints202604.0617.v1

In 2020, Janssen Pharmaceutica NV disclosed novel radiolabelled mGluR2/3 ligands for PET imaging and quantification of receptor expression in tissues [93]. Two fluorine-18 tracers, [^{18}F]-1 and [^{18}F]-2, were developed on the 5-phenyl-3-(pyridin-4-yl)-6,7-dihydropyrazolo[1,5-*a*]pyrazin-4(5*H*)-one scaffold (Figure 11). Binding studies with the corresponding non-radiolabelled analogues in Glu2-HEK293 and Glu3-HEK293 cells yielded pIC_{50} values of 8.1–8.8 and E_{max} values close to 100%. Both *ex vivo* biodistribution and PET scans showed that [^{18}F]-1 and [^{18}F]-2 achieved high brain uptake with low activity in the pons, a region lacking mGluR2/3 expression, consistent with receptor-specific binding. [^{18}F]-2 displayed rapid washout but suffered from extensive defluorination and bone uptake, whereas [^{18}F]-1 exhibited steadily increasing cortical and striatal activity, likely reflecting high affinity or pseudo-irreversible binding. In both cases, pretreatment with a reference NAM selective for mGluR2/3 reduced brain uptake to pons levels, confirming target specificity.

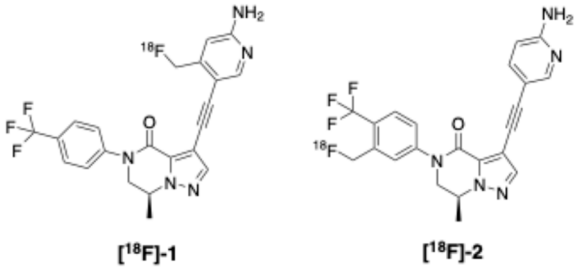

Figure 11. Structures of [^{18}F]-1 and [^{18}F]-2, radiolabelled mGluR2/3 tracers disclosed by Janssen Pharmaceutica NV in 2020 [93].

2.2.2. Metabotropic Glutamate Receptor 2 (mGluR2)

Research efforts have progressively shifted toward selective targeting of mGluR2 over mGluR3 to improve therapeutic outcomes. The development of PET radioligands targeting mGluR2 has evolved from early group II orthosteric antagonists, which showed several limitations—including poor BBB penetration, off-target binding, and interaction with efflux transporters—and restricted evaluation mainly to *in vitro* autoradiography or rodent imaging studies. These drawbacks prompted the shift toward allosteric modulators (AMs) as a more promising strategy. By engaging a binding site distinct from the conserved glutamate orthosteric pocket, AMs offer improved physicochemical properties and enhanced receptor selectivity. Allosteric PET tracers include both positive AMs (PAMs), which exhibit cooperativity in both affinity and efficacy with glutamate, and negative AMs (NAMs), which mainly affect efficacy. Notably, mGluR2 PAMs have been explored in the context of pain, schizophrenia, and drug addiction, while NAMs have been associated with cognitive disorders such as AD. Despite their potential, none of the mGluR2 PET tracers has yet reached clinical use. The only structurally disclosed tracer tested in humans, [^{11}C]JNJ-42491293, showed unexpected myocardial accumulation and off-target brain binding [94].

Following this line of research, a January 2023 published patent describes a new class of allosteric PET tracers based on the bicyclic structural scaffold of 3,4-dihydro-2*H*-pyrano[2,3-*b*]pyridine [95]. Two reference compounds emerged as suitable PET imaging candidates: 5-(2,4-difluorophenyl)-2,2-dimethyl-3,4-dihydro-2*H*-pyrano[2,3-*b*]pyridine-7-carboxamide (12, Figure 12) and 5-(2-fluoro-4-methoxyphenyl)-2,2-dimethyl-3,4-dihydro-2*H*-pyrano[2,3-*b*]pyridine-7-carboxamide (13, Figure 12). Both derivatives acted as potent mGluR2 NAMs (12: IC_{50}= 6 nM and 13: IC_{50}= 93.2 nM). Docking studies performed on an mGluR2 homology model confirmed the nanomolar affinity range, with stable allosteric poses stabilized by multiple hydrogen bonds and π–π interactions. Besides their mGluR2 binding, compounds 12 and 13 were also characterized for lipophilicity, plasma and microsomal stability, and interaction with P-glycoprotein (P-gp). Their physiochemical properties fell within the range associated with brain permeability, and the lack of P-gp interaction suggested favorable CNS pharmacokinetics. Prompted by these encouraging pharmacological and

 doi:10.20944/preprints202604.0617.v1

physicochemical profiles, compounds 12 and 13 were successfully radiolabeled, yielding the PET tracers [^{18}F]12 ([^{18}F]mG2N002) and [^{11}C]13, respectively (Figure 12) [95].

The first PET imaging study was carried out in Sprague Dawley rats, where [^{11}C]13 showed excellent brain permeability, with marked accumulation in mGluR2-rich regions such as the striatum, thalamus, cortex, hypothalamus, hippocampus, and cerebellum. The tracer displayed favorable kinetics, with most radioactivity cleared within 30 minutes, and a moderate-to-high level of specific binding, supporting its suitability as an mGluR2 PET probe. The second study was conducted in an AD mouse model, where [^{18}F]mG2N002 demonstrated excellent brain permeability and a heterogeneous yet consistent distribution across brain regions enriched in mGluR2. To further validate the potential of [^{11}C]13 as an imaging tool, a third study was conducted in non-human primates (cynomolgus monkeys), representing a pivotal translational approach for investigating the etiology of human neuropsychiatric disorders such as schizophrenia and drug addiction. [^{11}C]13 confirmed its ability to generate high-contrast images for mapping mGluR2 distribution in the primate brain. Kinetic analysis confirmed selective tracer accumulation in mGluR2-rich brain regions, which was markedly reduced after pretreatment with the selective NAM VU6001966, thereby validating target-specific binding. Consistent findings across rodent and primate studies provide strong evidence that [^{11}C]13, together with [^{18}F]mG2N002, are credible PET ligands for imaging mGluR2.

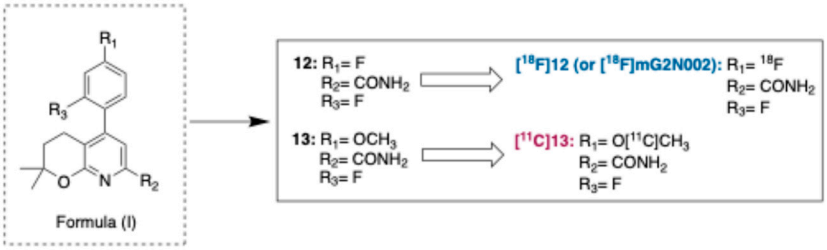

Figure 12. Chromane-based PET radioligands for mGluR2 imaging [95].

In 2021, Janssen Pharmaceutica NV revisited the class of 5-phenyl-3-(pyridin-4-yl)-6,7-dihydropyrazolo[1,5-*a*]pyrazin-4(5*H*)-ones previously disclosed in an earlier patent [93], introducing structural modifications to develop novel radiolabelled ligands selective for mGluR2 [96]. This invention covers a series of five compounds (Co. No. 1–5, Figure 13) along with their corresponding precursors (P, Figure 13), allowing conversion into radiotracers labeled with either ^{11}C or ^{18}F. Compounds 1–5 demonstrated potent NAM activity at human mGluR2 in the [^{35}S]GTPγS binding assay performed in the presence of glutamate. They showed pIC_{50} values in the range of 8.0–8.5 with E_{max} around 105–111%, and exhibited excellent selectivity over most mGluR subtypes, while discrimination against mGluR3 was more limited. Subsequent *in vivo* biodistribution studies in rats demonstrated that [^{11}C]-1 and [^{11}C]-2, derived from the precursors P-II and P-III (corresponding to Co. No. 1 and Co. No. 2, respectively; Figure 13), reached relatively high initial brain uptake at 2 min post-injection, followed by rapid clearance between 2 and 30 min. Although [^{11}C]-2 showed lower initial uptake than [^{11}C]-1, its washout was slightly slower, suggesting improved retention. *In vitro* autoradiography further confirmed high mGluR2 specificity, with [^{11}C]-2 emerging as the most promising candidate by displaying the highest specific-to-nonspecific binding ratios and strong blockade by reference NAMs. While no PET imaging data have yet been reported, the favorable preclinical profile of [^{11}C]-2 highlights its potential as a promising candidate for future *in vivo* evaluation.

 doi:10.20944/preprints202604.0617.v1

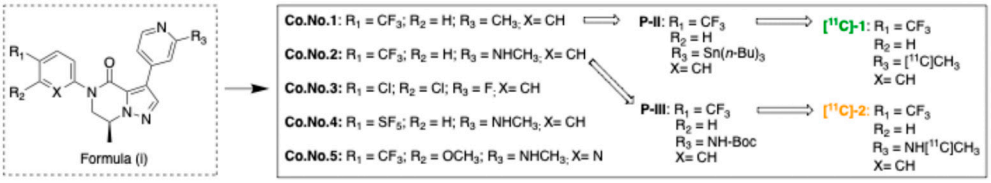

Figure 13. General scaffold of dihydropyrazolo[1,5-*a*]pyrazine derivatives from Janssen's mGluR2 tracer series, with representative examples [^{11}C]-1 and [^{11}C]-2 [96].

In the same year, another patent including a series of mGluR2 PAMs as PET ligands for investigating mGluR2-related pathophysiology at the molecular level was deposited by The General Hospital Corporation [97]. The application claims a broad series of benzimidazole-derived and related heterocyclic compounds, with radiolabeling achieved via one-step *O*-methylation of phenolic precursors using [^{11}C]CH_3I. Particular emphasis was given to compounds 1, 2, and 7 (Figure 14), which were profiled for molecular binding modes, pharmacology, physicochemical properties, and BBB permeability prior to *in vivo* evaluation, in order to mitigate the low and nonspecific brain uptake commonly observed with mGluR2 PET tracers. While all three derivatives showed solid profiles, compound 1 emerged as the most promising, combining nanomolar binding potency toward mGluR2 with excellent selectivity over other mGluRs, suitable lipophilicity and plasma protein binding, adequate metabolic stability, favorable passive permeability (PAMPA), and no P-gp liability. On this basis, compound 1 was selected for radiolabeling and subsequent *in vivo* evaluation as an mGluR2 PET radioligand. *Ex vivo* whole-body biodistribution of the [^{11}C]-*O*-methylated analogue of compound 1 ([^{11}C]1) showed rapid BBB penetration, combined hepatobiliary and renal clearance, and an overall pharmacokinetic profile consistent with use as a brain PET radioligand. *In vivo* PET studies in male Sprague-Dawley rats demonstrated time-dependent accumulation in mGluR2-rich regions, with the highest uptake in the thalamus, followed by striatum, cerebellum, and cortex. Specificity studies using a selective mGluR2 PAM from the same series confirmed target-specific binding, in line with the cAMP data on cold compound 1. Moreover, self-blocking with compound 1 increased tracer accumulation by up to 49%, a potentiating effect that may open new therapeutic perspectives for mGluR2-related psychiatric and neurological disorders.

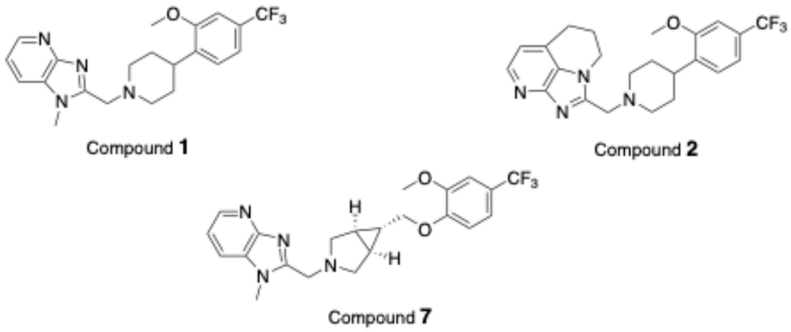

Figure 14. Representative pyridinimidazole-based compounds as mGluR2 PAMs and PET tracer candidates [97].

2.2.3. Metabotropic Glutamate Receptor 4 (mGluR4)

To further broaden the scope of metabotropic glutamate receptor imaging, in 2022 the General Hospital Corporation disclosed novel mGluR4 PAMs, proposed as allosteric PET imaging probes [98]. mGluR4 is broadly distributed at synapses within the basal ganglia, predominantly at presynaptic sites, and is also found in the striatum, hippocampus, thalamus, and cerebellum. Its activation suppresses GABA and glutamate release in basal ganglia circuits and reduces excitatory transmission in the cortex, thus drawing attention to it as a possible therapeutic target in PD. Consistently, several mGluR4 PAMs, including foliglurax (tested in phase II clinical trials), have

 doi:10.20944/preprints202604.0617.v1

shown antiparkinsonian effects in preclinical PD models. In parallel, although multiple mGluR4 PET tracers have been developed, most of them faced significant limitations, including chemical and metabolic instability, rapid clearance and short half-life, as well as suboptimal imaging contrast.

The present invention disclosed a series of picolinamide derivatives. Among them, compound 15 (Figure 15) stood out for its high mGluR4 affinity (IC_{50} = 3.4 nM) and PAM activity (EC_{50} = 324 nM), evaluated in the presence of an EC_{20} concentration of the reference agonist L-serine-*O*-phosphate (L-SOP) by monitoring intracellular cAMP levels. Selectivity was further assessed across different mGluR subtypes: mGluR1 and mGluR5 (G_q-coupled) were tested using Ca^{2+} mobilization assays, while mGluR2, mGluR3, mGluR4, mGluR6, and mGluR8 ($G_{i/o}$-coupled) were evaluated with cAMP assays. The results showed that compound 15 was selective over other mGluRs and displayed intrinsic mGluR4 agonist activity (EC_{50} = 2.75 μM), thereby classifying it as an mGluR4 ago-PAM, i.e., an allosteric modulator that exhibits intrinsic agonistic activity while enhancing the response to the endogenous ligand.

The *in vitro* pharmacological studies also showed that compound 15 possesses several CNS drug-like properties, including suitable lipophilicity and plasma protein binding, together with adequate metabolic and solution stability. Radiolabeling of compound 15 with fluorine-18 afforded [^{18}F]15 (Figure 15) in 10% radiochemical yield and 99% radiochemical purity, with a molar activity of 84.1 ± 11.8 GBq/μmol, likely influenced by the extended synthesis time. *Ex vivo* biodistribution studies demonstrated that the [^{18}F]15 displayed reversible binding across multiple tissues, including brain, liver, heart, lungs, and kidneys. *In vivo* PET imaging in male Sprague–Dawley rats confirmed brain accumulation in regions enriched with mGluR4. Pre-treatment with the corresponding non-labeled analogue 15 or with other mGluR4 allosteric ligands produced dose-dependent reductions in tracer uptake, confirming specific receptor binding. Collectively, these findings support the potential of [^{18}F]15 as a PET imaging probe for disorders involving mGluR4 dysfunction, such as PD.

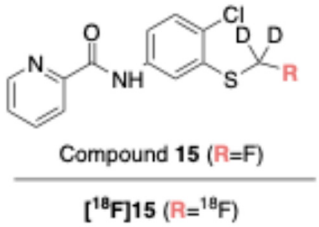

Figure 15. Chemical structure of [^{18}F]15 as an exemplary PET radioligand for mGluR4 [98].

2.2.4. Dopamine D1 Receptor (D1R)

Dopaminergic neurotransmission plays a key role in human brain being involved in movement, cognition and reward behavior. Five dopamine receptor subtypes (D1R-D5R) are known, and they have been classified into two major GPCR families. D1-like receptors (D1R and D5R) are primarily postsynaptic and preferentially couple to G_s proteins, leading to increased cAMP production, whereas D2-like receptors (D2R, D3R, and D4R) are expressed both pre- and postsynaptically and mainly signal through $G_{i/o}$ proteins, resulting in reduced cAMP levels [99,100]. They are widely expressed across multiple brain regions: D1-like receptors are mostly found in the caudate–putamen (*striatum*), nucleus accumbens, *substantia nigra pars reticulata*, olfactory bulb, amygdala, and frontal cortex [101,102]. Accordingly, D1-like receptors are implicated in a variety of disorders, including negative symptoms in schizophrenia, attention-deficit/hyperactivity disorder (ADHD), PD and related movement disorders, dementia and AD, age-related cognitive decline, sleep disorders, and apathy. D2-like receptors are mainly expressed in *striatum*, the lateral part of the *globus pallidus*, core of the nucleus accumbens, ventral tegmental area, hypothalamus, amygdala, cortical areas, hippocampus, and pituitary [101,103]. While also involved in motor regulation (e.g., Huntington's Disease (HD) and dystonia), D2-like receptors are more closely linked to schizophrenia (positive

 doi:10.20944/preprints202604.0617.v1

symptoms), reward-related disorders such as addiction, and endocrine dysregulation, particularly hyperprolactinemia.

From a pharmacological perspective, the high degree of homology within the ligand-binding site among D1- and D2-like receptor subtypes poses a major challenge, as it often results in limited selectivity and off-target effects of existing drugs. This issue is further amplified in the development of PET imaging agents, where achieving high subtype selectivity is of critical relevance [104]. PET imaging agents developed so far for dopaminergic receptor subtypes are mainly based on agonists or, alternatively, antagonists; however, they are affected by several limitations, including insufficient subtype selectivity, suboptimal pharmacokinetic properties, and the generation of radioactive metabolites. The recent patent activity of UCB Biopharma S.R.L. has aimed to overcome these limitations by disclosing radiolabelled 6-[2-(fluoromethyl)-4-(furo[3,2-c]pyridin-4-yloxy)phenyl]-1,5-dimethylpyrimidine-2,4(1*H*,3*H*)-dione compounds, which act as selective D1-like PET imaging agents [105]. In detail, the present invention relates to compounds of formula (±)-I, existing as a mixture of two atropisomers (Figure 16), wherein at least one hydrogen atom is replaced by tritium (^{3}H), the *N*-methyl group is labelled with ^{11}C, or the fluorine atom is ^{18}F. Compounds of formula (±)-I act as selective ligands for D1-like receptors, displaying high affinity for the human D5R (pK_i = 9.4) and exhibiting more than 1000-fold selectivity over the other 79 targets tested. Preclinical studies described in the patent show that the proposed D1-like PET tracers exhibit high and displaceable striatal binding in non-human primate brain, consistent with D1R distribution. *In vivo* PET imaging demonstrated favorable brain kinetics, quantifiable specific binding in the caudate and putamen, and a metabolite profile dominated by hydrophilic species unlikely to cross the BBB. Importantly, tracer uptake was markedly enhanced by co-administration of a D1R PAM, highlighting the suitability of these ligands for imaging D1R function. Although the compounds shown in Figure 16 act at the orthosteric site, these findings support the broader concept that allosteric modulation can provide an additional layer of selectivity for dopaminergic PET imaging, potentially overcoming limitations associated with the highly conserved orthosteric binding site.

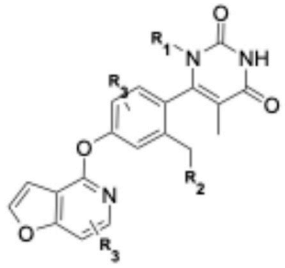

Compound (±)-I: $R_1 = CH_3$; $R_2 = F$; $R_3 = H$
Compound (±)-Ia: $R_1 = [^{11}C]CH_3$; $R_2 = F$; $R_3 = H$
Compound (±)-Ib: $R_1 = CH_3$; $R_2 = [^{18}F]F$; $R_3 = H$
Compound (±)-Ic: $R_1 = CH_3$; $R_2 = F$; $R_3 = [^{3}H]$ (at least one tritium atom)

Figure 16. Structure of compound (±)-I, shown as a mixture of two atropisomers and alternatively radiolabeled with ^{11}C ((±)-Ia), ^{18}F ((±)-Ib), or ^{3}H ((±)-Ic), disclosed by UCB Biopharma S.R.L. as D1-like PET imaging agents [105].

2.3. Inflammatory Diseases

Inflammation is involved in many diseases, from immune-mediated disorders like rheumatoid arthritis (RA) to more common conditions such as cardiovascular disease and diabetes, beyond its close association with multiple aspects of tumor progression. As such, inflammation poses a significant diagnostic challenge, characterized by poorly defined clinical endpoints, high inter-patient variability, systemic involvement, and non-specific clinical or laboratory features. An example of this complexity is the potential mismatch between disease manifestation and treatment distribution, as observed in a pathology like RA that affects multiple tissues [106].

 doi:10.20944/preprints202604.0617.v1

Consequently, the role of nuclear medicine in both the diagnostic workup and the therapeutic follow-up of these conditions has expanded considerably in recent years. Currently, the mainstay of inflammation imaging is [^{18}F]FDG-PET/CT, routinely applied to a broad range of disorders, such as large-vessel vasculitis, sarcoidosis, and spondylodiscitis. However, its intrinsic limitation lies in the lack of specificity, since increased glycolytic uptake is also observed in malignant lesions and in *sterile* inflammatory processes [107,108].

Beyond immunoPET — which combines the high specificity and selectivity of monoclonal antibodies and engineered derivatives with the sensitivity and quantitative capabilities of PET imaging and is therefore increasingly at the forefront of clinical practice for several conditions, including inflammatory diseases — there is growing consensus that host-targeted approaches, such as GPCR-targeted tracers, may represent a relevant step forward to improve specificity in molecular imaging of inflammation [109,110]. After all, it is well known that GPCRs play key roles in inflammation, as they translate inflammatory states into molecular signals [111]. This makes them highly informative biomarkers for molecular imaging, offering the opportunity to decipher functional inflammatory pathways rather than merely detecting inflammatory burden. Consistent with this, tracers targeting chemokine-axis GPCRs are of particular interest.

2.3.1. CC Chemokine Receptor 2 (CCR2)

In June 2024, a patent disclosed what is described as the first imaging probe developed for CC-chemokine receptor 2 (CCR2) [112]. CCR2 is a GPCR of the chemokine receptor family, primarily expressed on monocytes, immature dendritic cells and specific T-cell subsets, where it mediates chemotactic migration to sites of inflammation in response to endogenous ligands such as CCL2 [113]. The CCL2/CCR2 axis is essential for the recruitment of pro-inflammatory monocytes from hematopoietic sites to inflamed tissues; upon ligand stimulation, CCR2^{+} monocytes adhere to the endothelium and give rise to macrophages or dendritic cells, thereby amplifying local inflammatory responses through the release of pro-inflammatory mediators. Dysregulated or sustained activation of this pathway is implicated in a wide range of diseases, including inflammatory pain, atherosclerosis, neuroinflammatory disorders, RA and diabetic nephropathy.

It is worth noting that elevated levels of CCL2 and infiltration of CCR2^{+} immune cells are characteristic of acute and chronic lung diseases, including acute respiratory distress syndrome (ARDS), chronic obstructive pulmonary disease (COPD), experimental asthma, and pulmonary fibrosis. Together, these features make CCR2 a highly attractive molecular target for inflammation imaging, supporting the growing interest in the development of dedicated CCR2 imaging probes for both pre-clinical and clinical applications.

Therefore, the applicants adapted the CCR2-binding peptide ECL1i (D-Leu-Gly-D-Thr-D-Phe-D-Leu-D-Lys-D-Cys) as a molecular imaging probe for PET. Two CCR2-targeted imaging agents were developed: a monovalent ^{64}Cu-radiolabeled peptide (^{64}Cu-DOTA-ECL1i, Figure 17) and a multivalent nanostructured probe consisting of ECL1i conjugated to copper-doped gold nanoclusters (^{64}CuAuNCs-ECL1i).

The authors demonstrated that peptide ECL1i enables specific *in vivo* PET/CT imaging of CCR2 in ischemia–reperfusion injury following lung transplantation, both as a monovalent peptide tracer and a multivalent nanoplatform. However, owing to their distinct pharmacokinetic profiles, ^{64}Cu-DOTA-ECL1i is reported to be more suitable for rapid and serial CCR2 imaging, whereas the multivalent ^{64}CuAuNCs-ECL1i, characterized by extended pharmacokinetics, is favored for long-term CCR2 detection and potential targeted theranostic applications.

To explore the ability to image CCR2-associated inflammation, ^{64}Cu-DOTA-ECL1i was tested in LPS-induced lung injury, where its uptake increased during the acute phase only, with no signal detected in CCR2-deficient mice and complete blockade upon co-administration of non-radioactive ECL1i.

Beyond data including tests of ^{64}Cu-DOTA-ECL1i specificity, sensitivity, and safety in mouse models of lung injury to validate radiotracer performance, the patent also reports *ex vivo* validation

 doi:10.20944/preprints202604.0617.v1

of CCR2 targeting in human tissues. Autoradiography on lung sections demonstrated markedly increased ^{64}Cu-DOTA-ECL1i binding in samples from patients with COPD compared with normal donor tissues, consistent with increased CCR2 expression.

The patent further reports preclinical toxicology and dosimetry studies in animals, alongside the establishment of chemistry, manufacturing, and controls (CMC) documentation and standard operating procedures for ^{64}Cu-DOTA-ECL1i. These activities are described as preparatory steps toward an exploratory IND application, thereby supporting the translational potential of the tracer.

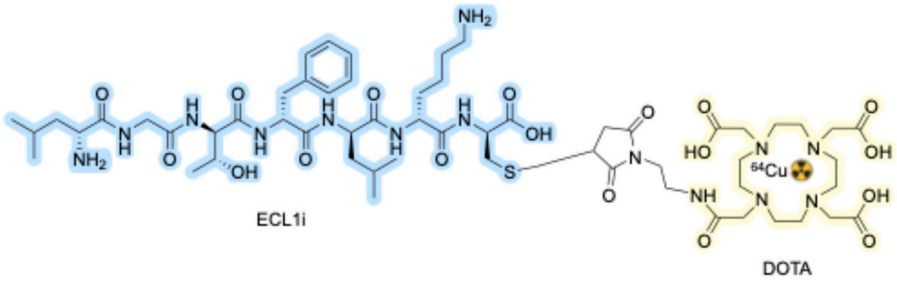

Figure 17. Chemical structure of ^{64}Cu-DOTA-ECL1i [112].

2.3.2. CXC Chemokine Receptor 2 (CXCR2)

The human CXC chemokine receptor 2 (CXCR2) is a GPCR involved in neutrophil-driven inflammatory responses. Neutrophils are key effectors of innate immunity, playing a central role in phagocytic host defense. Accordingly, variations in neutrophil recruitment and activation represent important biomarkers that can be quantified and correlated with disease presence and progression [114,115].

Researchers at University of Würzburg have reported the first PET radiotracer targeting CXCR2, outlining its potential *in vivo* application for imaging CXCR2-mediated pathologies. These may include inflammatory conditions characterized by neutrophil recruitment, such as cancer, ischemic injury, bowel disease, respiratory disorders, atherosclerosis, and selected autoimmune or degenerative diseases [116]. The patent describes the development of fluorinated analogues based on a squaramide scaffold (general formula shown in Figure 18), obtained through exploration of different substitution sites and synthetic strategies. SAR analysis highlighted the critical role of hydrogen-bond donors in receptor recognition, with the aliphatic side chain of one donor being essential for maintaining CXCR2 selectivity, while a broad range of aliphatic and aromatic substitutions on the right-hand side were tolerated without significant loss of affinity. The resulting compounds were evaluated *in vitro*, leading to the identification of compound 3b as the most suitable tracer candidate. In parallel, only a modest enantioselective preference was observed, as the (*R*)-enantiomer of 3b (IC_{50} = 273 nM) slightly outperformed the corresponding (*S*)-enantiomer (IC_{50} = 428 nM). Thus, the ^{18}F-labeled analogue of (*R*)-3b was selected for further development. Cell uptake studies demonstrated that [^{18}F]-(*R*)-3b (Figure 18) exhibited time-dependent and CXCR2-specific accumulation in CXCR2-overexpressing HEK293 cells, which was effectively blocked by a reference CXCR2 antagonist. Tracer uptake was observed exclusively in CXCR2-positive cells, confirming high target specificity and highlighting the potential of [^{18}F]-(*R*)-3b for functional imaging of neutrophils in inflammatory diseases. These findings were further corroborated in human peripheral blood neutrophils, where target specificity was again confirmed by antagonist blockade.

Initial microPET studies showed rapid clearance from most organs, short liver retention, and predominant renal excretion. Notably, negligible bone uptake—commonly associated with *in vivo* defluorination—indicated high metabolic stability. Collectively, these data provided key information for dosimetry estimation and the establishment of clinical imaging protocols.

 doi:10.20944/preprints202604.0617.v1

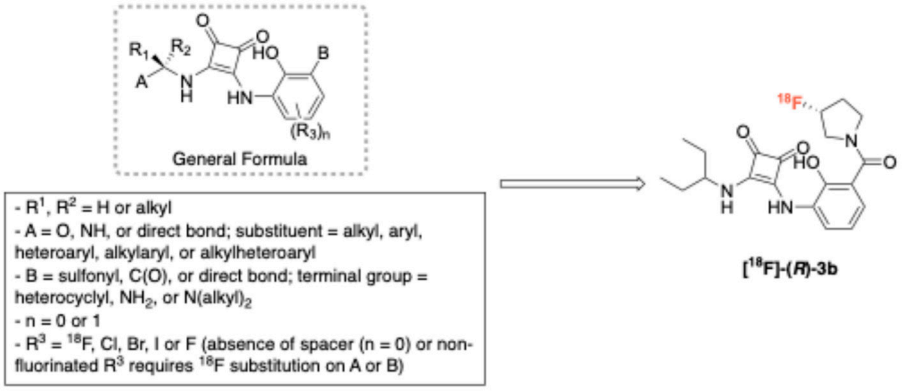

Figure 18. Structure of the first ^{18}F-labeled CXCR2 PET tracer (right) together with the general formula (left) of its chemical class [116].

2.3.3. CXC Chemokine Receptor Type 4 (CXCR4)

CXCR4, previously discussed as a key molecular imaging target in oncology, has also emerged as a highly relevant target in inflammatory diseases due to its pivotal role in chemotaxis and leukocyte trafficking. In RA, the SDF-1/CXCR4 signaling axis mediates the pro-inflammatory migration of activated T cells to sites of inflammation; accordingly, synovial tissues from RA patients show increased infiltration of T cells with elevated CXCR4 expression [117]. Beyond autoimmune disorders, dysregulation of the SDF-1/CXCR4 axis also contributes to cardiovascular inflammatory pathologies. In the early stages of atherosclerosis, SDF-1/CXCR4 signaling promotes the recruitment of endothelial progenitor cells to sites of vascular injury, thereby participating in plaque formation, although some evidence suggests a potential atheroprotective role. Notably, atherosclerotic plaques are characterized by hypoxic microenvironments, which are known to upregulate CXCR4 expression and modulate immune cell trafficking. Accordingly, PET diagnostic agents targeting CXCR4 may provide valuable prognostic information in atherosclerosis [118]. On the whole, these observations highlight a significant unmet need for improved imaging agents and radiotherapeutic compositions enabling *in vivo* PET diagnosis and treatment not only of cancer but also of inflammatory/autoimmune diseases characterized by CXCR4 overexpression.

To the best of our knowledge, CXCR4-targeted imaging agents have been developed based on radiolabeled monoclonal antibodies, cyclam-derived inhibitors, and peptides. More recently, applicants from The University of British Columbia disclosed novel CXCR4-targeting radiopharmaceuticals derived from the cyclic peptide LY2510924 (cyclo[Phe-Tyr-Lys(iPr)-D-Arg-2-Nal-Gly-D-Glu]-Lys(iPr)-NH_2), a potent CXCR4 antagonist capable of blocking SDF-1α binding with nanomolar affinity. These agents were extensively evaluated in PET studies using CXCR4-expressing malignancy models; however, the authors also claim their use for imaging inflammatory and autoimmune conditions [119,120].

2.3.4. G protein-Coupled Receptor 84 (GPR84)

Among the GPCRs attracting increasing attention, the orphan receptor GPR84 has emerged as a promising PET imaging biomarker of detrimental innate immune activation. While its basal expression on pro-inflammatory myeloid cells such as macrophages, microglia, and neutrophils is low, it becomes strongly upregulated in response to CNS injury or inflammatory stimuli. To validate GPR84's potential, a patent application filed in October 2024 by The Board of Trustees of the Leland Stanford Junior University disclosed the design and synthesis of ^{11}C-labeled PET tracers for the selective imaging of neurological and inflammatory-related diseases associated with GPR84 expression [121]. The tracer selection was guided by prior research on (1,4-dioxan-2-ylmethoxy)-6,7-dihydropyrimido[6,1-*a*]isoquinolin-4-one (DDHPI) compounds (general formula in Figure 19), identified as potent and selective GPR84 NAMs [122]. Among the candidates, compounds with favorable physicochemical features for ^{11}C-labeling and CNS penetration—such as molecular weight,

 doi:10.20944/preprints202604.0617.v1

topological polar surface area (TPSA), and lipophilicity—were prioritized. This led to the selection of MGX-10S and MGX-11S, which displayed low-nanomolar binding affinity in competitive assays with ^{3}H-G9543, a reference GPR84 inhibitor. Functional cAMP and ^{35}S-GTPγS assays confirmed target engagement, showing moderate-to-high nanomolar IC_{50} values, consistent with strong binding but limited inhibitory activity, a profile considered suitable for PET tracers. The non-labeled analogues (MGX-8S and MGX-9S) were synthesized as HPLC standards for radiotracer identification and subsequently radiolabeled to obtain ^{11}C-MGX-10S and ^{11}C-MGX-11S. *In vitro* assays in *h*GPR84-HEK293 cells demonstrated that ^{11}C-MGX-10S displayed higher specificity than ^{11}C-MGX-11S, with binding effectively blocked by the reference antagonist GLPG1205. In mice, both tracers crossed the BBB, but ^{11}C-MGX-10S exhibited superior brain uptake and more favorable washout kinetics, prompting its further evaluation in a model of innate immune activation. In this setting, ^{11}C-MGX-10S proved metabolically stable, remaining largely intact in the brain even under inflammatory conditions. PET imaging in LPS-treated mice revealed elevated ^{11}C-MGX-10S uptake in the brain, liver, and intestines compared to controls, with increased binding across most brain regions, consistent with GPR84 upregulation in inflammation. Pre-treatment with the antagonist GLPG1205 significantly reduced tracer accumulation, confirming binding specificity, while *ex vivo* analyses supported the *in vivo* findings. Importantly, when compared with the TSPO tracer ^{11}C-DPA-713, ^{11}C-MGX-10S showed a superior signal-to-background ratio, underscoring its potential for sensitive detection of inflamed tissues.

Overall, this elegant patent has led to the development of ^{11}C-MGX-10S as a highly specific GPR84 radiotracer, showcasing its strong *in vivo* stability, selective binding, and enhanced uptake in inflamed brain regions, positioning it as a valuable tool for neuroinflammation and innate immune activation imaging.

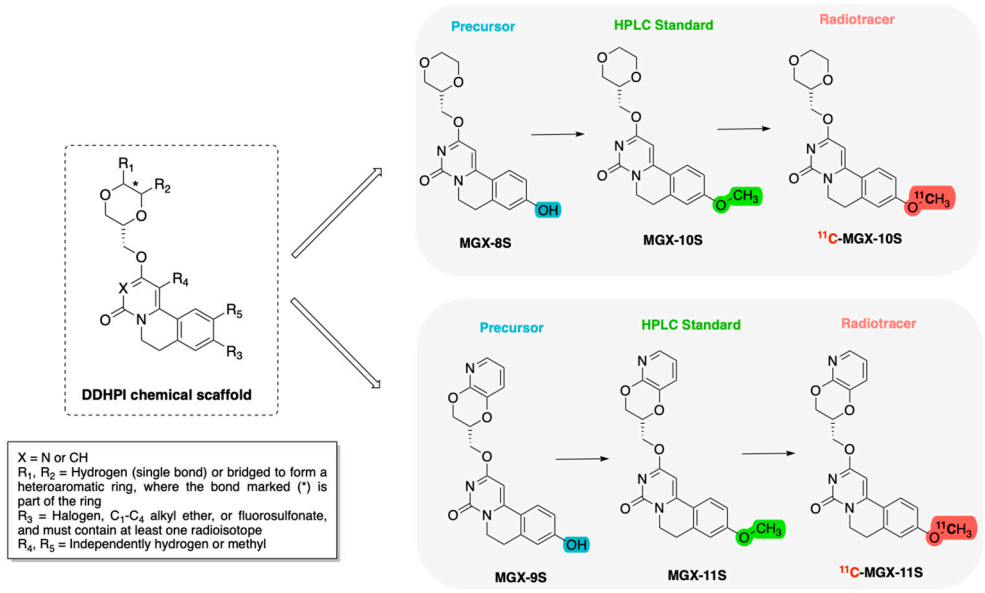

Figure 19. General formula of (1,4-dioxan-2-ylmethoxy)-6,7-dihydropyrimido[6,1-*a*]isoquinolin-4-one (DDHPI) derivatives patented as GPR84 radioligands. Representative radiotracers ^{11}C-MGX-10S and ^{11}C-MGX-11S together with their corresponding HPLC standards (MGX-10S, MGX-11S) and precursors (MGX-8S, MGX-9S) [122].

3. Discussion

The last five years have been characterized by an intense patent activity in the field of GPCR-targeted PET radiotracers. A critical analysis of the reviewed patents reveals primarily a recurrent *a posteriori* design strategy, whereby established GPCR ligands are adapted to PET imaging rather than conceived as *de novo* radiotracers. In many cases, development starts from known drugs, tool

 doi:10.20944/preprints202604.0617.v1

compounds, or clinically validated vectors, which have been modified to enable radiolabeling and then evaluated for their suitability as imaging agents.

This pattern is consistently observed across multiple targets. For instance, US2023099200A1 uses R54 as a structural template for the development of CXCR4-targeted tracers [62]. Similarly, US20230270893 relies on a clinically mature ligand (PP-F11N) to develop a specific PET imaging agent for CCKBR-positive tumors. Along the same lines, WO2025008409 discloses novel radiometal-based derivatives inspired by the well-known NK1R antagonist aprepitant [67]. Collectively, these examples illustrate a pragmatic and translationally oriented approach, in which prior knowledge of target engagement and *in vivo* behavior is leveraged to reduce development risk. Accordingly, the central design objective is the meticulous preservation of target affinity and selectivity while imposing the physicochemical and biological constraints required for successful PET imaging, including metabolic stability, clearance profile, and—where relevant—CNS penetration. Clear examples of this (radio)medicinal chemistry–driven rationale can be found in the development of chromane-based PET radioligands for mGluR2 imaging, where candidate selection follows a structured workflow encompassing binding mode analysis and stringent filtering based on lipophilicity, metabolic stability, and P-gp liability prior to radiolabeling and *in vivo* validation [95]. Similarly, the development of GPR84 PET tracers relies on the prioritization of compounds meeting the physicochemical requirements for CNS penetration, including molecular weight, TPSA, and lipophilicity compatible with brain imaging [121].

A careful analysis of patented imaging agents reveals the recurrent adoption of specific structural motifs that appear to be key determinants of *in vivo* performance, translational robustness, and theranostic potential. Across different disease areas and GPCR subclasses, several convergent design principles emerge.

Peptide-based radiotracers continue to dominate oncology-oriented patents, such as those targeting SSTRs, CCK2R, CXCR4, and KISS1R. Only a few small-molecule ligands emerge as exceptions within this peptide-dominated landscape, particularly those targeting NK1R [67] and NTSR1 [84].

Generally, conformational constraints (e.g., cyclization, disulfide bridges, and incorporation of non-natural amino acids) are repeatedly exploited to enhance receptor selectivity by restricting conformational flexibility and stabilizing bioactive binding geometries, thereby reducing off-target interactions with closely related GPCR subtypes. Moreover, these features may also contribute to improved resistance to proteolytic degradation, supporting more favorable *in vivo* stability.

Beyond this local level of structural control, many of the patents examined point to a complementary design logic with a strong emphasis on modular architectures. This tendency is particularly evident in metal-based radiopharmaceuticals, which frequently adopt a conserved M*–C–L–V organization, where the radiometal (M*) is coordinated by a chelator (C) and connected to the targeting vector (V) through a dedicated linker (L). Within this framework, modularity arises from the functional decoupling of target engagement, pharmacokinetic behavior, and radiochemical properties, enabling the individual components to be adapted within a conserved molecular scaffold to suit the intended application. This can be seen, for example, in access to a wide spectrum of physical half-lives, not only among PET radiometals—such as ^{68}Ga, which is well suited for fast-diffusing targeting vectors including peptides—but also among longer-lived isotopes, such as ^{64}Cu and ^{89}Zr, which are preferred for carriers requiring prolonged circulation times to reach the tumor site, including monoclonal antibodies. Importantly, the same molecular platforms can be extended to therapeutic applications through labeling with α-emitters (e.g. ^{225}Ac) or β-emitters (e.g. ^{177}Lu). This trend is clearly reflected in the oncology-focused patents that we looked at, where traditional PET radionuclides like ^{11}C and ^{18}F are increasingly being replaced by, for example, ^{68}Ga. On that note, the growing interest in ^{68}Ga is driven by its good coordination chemistry, which enables the formation of highly stable macrocyclic chelates, as well as by its simplified production via ^{68}Ge/^{68}Ga generators, independent of on-site cyclotron facilities. Moreover, ^{68}Ga forms a matched theranostic pair with

 doi:10.20944/preprints202604.0617.v1

^{177}Lu, enabling ^{68}Ga-based imaging to support patient selection and treatment planning prior to ^{177}Lu-based radiotherapy.

In contrast, the design of radiotracers for CNS imaging strongly favors drug-like molecular architectures. Successful CNS PET tracer development consistently adheres to classical ADME-driven constraints—such as optimized lipophilicity, TPSA, and conformational rigidity—closely mirroring the criteria applied to CNS-active drugs. Accordingly, well-established heteroaromatic and polycyclic scaffolds, including pyridinimidazoles, chromans, pyridinecarboxamides, and condensed bicyclic pyrazolo–pyrazine cores, are recurrently employed.

Within this framework, the dominant design constraints revolve around minimal structural perturbation upon radiolabeling, careful control of lipophilicity, and preservation of BBB permeability. Consequently, radionuclide selection remains largely anchored to traditional isotopes such as ^{11}C and ^{18}F, favoring straightforward covalent labeling strategies (e.g., ^{18}F-C bond formation).

The CNS imaging patent landscape reflects a mature and increasingly sophisticated view of GPCR biology. Several patents emphasize allosteric or non-competitive binding modes [95,98] or dual-targeting strategies [57], reflecting a growing interest in interrogating GPCR functional and signaling states rather than receptor density alone. This clearly shows the intention to evolve the field of GPCR-targeted PET imaging towards increasingly functional and mechanism-oriented applications. Future radiotracers will likely be gradually called upon to consolidate their strategic role as companion tools in drug development, supporting target validation, dose selection, and go/no-go decisions.

In addition to oncological and CNS applications, PET imaging targeting GPCRs in inflammatory disorders is an attractive, yet still largely underexplored, area. Inflammation-related PET imaging biomarkers offer unique opportunities to capture dynamic cellular activation and microenvironmental changes *in vivo* and may represent a unifying imaging axis across oncology and CNS, given the central role of inflammatory processes—either immune-driven or arising from non-immune tissue stress—in both tumor progression and neuroinflammatory disorders. This key strength of inflammation imaging aligns particularly well with GPCRs, whose biology is intrinsically linked to inflammatory signaling and immune-related mechanisms, thereby enabling a truly cross-cutting biomarker role. Established examples include GPCRs used as inflammatory imaging biomarkers, such as chemokine receptors from the CC and CXC families, which also serve as biomarkers of tumor behavior. More recently identified GPCRs, such as GPR65, have further expanded this concept, with GPR65 being reported as a novel immune-related biomarker whose role in regulating tumor-associated inflammatory responses could confer both prognostic and diagnostic relevance in lung adenocarcinoma [123].

Therefore, the limited number of patent filings related to GPCR-targeted probes for inflammation imaging is not due to a lack of biological relevance, but rather to the intrinsic complexity of inflammatory processes that are finely tuned systems. Nevertheless, as our understanding of inflammation biology continues to evolve and imaging strategies increasingly shift toward functional readouts, GPCR-targeted molecular imaging is well positioned to deliver mechanistic and clinically relevant insights across inflammatory, oncological, and CNS–related conditions.

Author Contributions: Conceptualization, R.F.; methodology, R.F., and C.D.; validation, C.D.; formal analysis, R.F. and C.P.; investigation, R.F., and C.M.; data curation, R.F., and C.M.; writing—original draft preparation, R.F.; writing—review and editing, C.M., A.C., M.D.A., C.P. and C.D.; visualization, R.F., C.M. and A.C.; supervision, R.F., M.D.A. and C.D. All authors have read and agreed to the published version of the manuscript.

Funding: This research received no external funding.

Data Availability Statement: Not applicable.

Acknowledgments: The authors acknowledge Fondazione Cariplo (Project No. 2024-0984), which supports research on GPCR-targeted PET tracer development.

 doi:10.20944/preprints202604.0617.v1

Conflicts of Interest: The authors declare no conflicts of interest.

References

1. Ametamey, S.M.; Honer, M.; Schubiger, P.A. Molecular Imaging with PET. *Chem. Rev.* **2008**, *108*, 1501–1516, doi:10.1021/cr0782426.
2. Phelps, M.E. Positron Emission Tomography Provides Molecular Imaging of Biological Processes. *Proc. Natl. Acad. Sci.* **2000**, *97*, 9226–9233, doi:10.1073/pnas.97.16.9226.
3. Miller, P.W.; Long, N.J.; Vilar, R.; Gee, A.D. Synthesis of ^{11}C, ^{18}F, ^{15}O, and ^{13}N Radiolabels for Positron Emission Tomography. *Angew. Chem. Int. Ed.* **2008**, *47*, 8998–9033, doi:10.1002/anie.200800222.
4. Halder, R.; Ritter, T. ^{18}F-Fluorination: Challenge and Opportunity for Organic Chemists. *J. Org. Chem.* **2021**, *86*, 13873–13884, doi:10.1021/acs.joc.1c01474.
5. Coenen, H.H.; Elsinga, P.H.; Iwata, R.; Kilbourn, M.R.; Pillai, M.R.A.; Rajan, M.G.R.; Wagner, H.N.; Zaknun, J.J. Fluorine-18 Radiopharmaceuticals beyond [18F]FDG for Use in Oncology and Neurosciences. *Nucl. Med. Biol.* **2010**, *37*, 727–740, doi:10.1016/j.nucmedbio.2010.04.185.
6. Goud, N.S.; Bhattacharya, A.; Joshi, R.K.; Nagaraj, C.; Bharath, R.D.; Kumar, P. Carbon-11: Radiochemistry and Target-Based PET Molecular Imaging Applications in Oncology, Cardiology, and Neurology. *J. Med. Chem.* **2021**, *64*, 1223–1259, doi:10.1021/acs.jmedchem.0c01053.
7. Rong, J.; Haider, A.; Jeppesen, T.E.; Josephson, L.; Liang, S.H. Radiochemistry for Positron Emission Tomography. *Nat. Commun.* **2023**, *14*, 3257, doi:10.1038/s41467-023-36377-4.
8. Yordanova, A.; Eppard, E.; Kürpig, S.; Bundschuh, R.; Schönberger, S.; Gonzalez-Carmona, M.; Feldmann, G.; Ahmadzadehfar, H.; Essler, M. Theranostics in Nuclear Medicine Practice. *OncoTargets Ther.* **2017**, *Volume 10*, 4821–4828, doi:10.2147/OTT.S140671.
9. Abikhzer, G.; Treglia, G.; Pelletier-Galarneau, M.; Buscombe, J.; Chiti, A.; Dibble, E.H.; Glaudemans, A.W.J.M.; Palestro, C.J.; Sathekge, M.; Signore, A.; et al. EANM/SNMMI Guideline/Procedure Standard for [18F]FDG Hybrid PET Use in Infection and Inflammation in Adults v2.0. *Eur. J. Nucl. Med. Mol. Imaging* **2025**, *52*, 510–538, doi:10.1007/s00259-024-06915-3.
10. Been, L.B.; Suurmeijer, A.J.H.; Cobben, D.C.P.; Jager, P.L.; Hoekstra, H.J.; Elsinga, P.H. [18F]FLT-PET in Oncology: Current Status and Opportunities. *Eur. J. Nucl. Med. Mol. Imaging* **2004**, *31*, 1659–1672, doi:10.1007/s00259-004-1687-6.
11. Dunet, V.; Rossier, C.; Buck, A.; Stupp, R.; Prior, J.O. Performance of ^{18}F-Fluoro-Ethyl-Tyrosine (^{18}F-FET) PET for the Differential Diagnosis of Primary Brain Tumor: A Systematic Review and Metaanalysis. *J. Nucl. Med.* **2012**, *53*, 207–214, doi:10.2967/jnumed.111.096859.
12. Araz, M.; Aras, G.; Küçük, Ö.N. The Role of 18F–NaF PET/CT in Metastatic Bone Disease. *J. Bone Oncol.* **2015**, *4*, 92–97, doi:10.1016/j.jbo.2015.08.002.
13. Derlin, T.; Richter, U.; Bannas, P.; Begemann, P.; Buchert, R.; Mester, J.; Klutmann, S. Feasibility of ^{18}F-Sodium Fluoride PET/CT for Imaging of Atherosclerotic Plaque. *J. Nucl. Med.* **2010**, *51*, 862–865, doi:10.2967/jnumed.110.076471.
14. Evans, J.D.; Jethwa, K.R.; Ost, P.; Williams, S.; Kwon, E.D.; Lowe, V.J.; Davis, B.J. Prostate Cancer–Specific PET Radiotracers: A Review on the Clinical Utility in Recurrent Disease. *Pract. Radiat. Oncol.* **2018**, *8*, 28–39, doi:10.1016/j.prro.2017.07.011.
15. Parihar, A.S.; Vaz, S.; Sutcliffe, S.; Pant, N.; Schoones, J.W.; Ulaner, G.A. ^{18}F-Fluoroestradiol PET/CT for Predicting Benefit from Endocrine Therapy in Patients with Estrogen Receptor–Positive Breast Cancer: A Systematic Review and Metaanalysis. *J. Nucl. Med.* **2025**, *66*, 692–699, doi:10.2967/jnumed.124.269163.
16. Dhawan, V.; Niethammer, M.H.; Lesser, M.L.; Pappas, K.N.; Hellman, M.; Fitzpatrick, T.M.; Bjelke, D.; Singh, J.; Quatarolo, L.M.; Choi, Y.Y.; et al. Prospective F-18 FDOPA PET Imaging Study in Human PD. *Nucl. Med. Mol. Imaging* **2022**, *56*, 147–157, doi:10.1007/s13139-022-00748-4.
17. Mattay, V.S.; Fotenos, A.F.; Ganley, C.J.; Marzella, L. Brain Tau Imaging: Food and Drug Administration Approval of ^{18}F-Flortaucipir Injection. *J. Nucl. Med.* **2020**, *61*, 1411–1412, doi:10.2967/jnumed.120.252254.
18. Zürcher, N.R.; Walsh, E.C.; Phillips, R.D.; Cernasov, P.M.; Tseng, C.-E.J.; Dharanikota, A.; Smith, E.; Li, Z.; Kinard, J.L.; Bizzell, J.C.; et al. A Simultaneous [11C]Raclopride Positron Emission Tomography and

 doi:10.20944/preprints202604.0617.v1

Functional Magnetic Resonance Imaging Investigation of Striatal Dopamine Binding in Autism. *Transl. Psychiatry* **2021**, *11*, 33, doi:10.1038/s41398-020-01170-0.

19. Youn, Y.C.; Jang, J.-W.; Han, S.-H.; Kim, H.; Seok, J.W.; Byun, J.S.; Park, K.-Y.; An, S.S.; Chun, I.K.; Kim, S. ^{11}C-PIB PET Imaging Reveals That Amyloid Deposition in Cases with Early-Onset Alzheimer’s Disease in the Absence of Known Mutations Retains Higher Levels of PIB in the Basal Ganglia. *Clin. Interv. Aging* **2017**, *Volume 12*, 1041–1048, doi:10.2147/CIA.S132884.
20. Grassi, I.; Nanni, C.; Allegri, V.; Morigi, J.J.; Montini, G.C.; Castellucci, P.; Fanti, S. The Clinical Use of PET with 11C-Acetate.
21. Singh, H.; Bhasin, D.; Gunasekaran, V.; Subedi, U.; Mittal, B.R. Potential Role of 13N-NH3 Cardiac PET in Monitoring Treatment Response in Patients with Microvascular Angina. *Indian J. Nucl. Med.* **2025**, *40*, 103–105, doi:10.4103/ijnm.ijnm_16_25.
22. Slart, R.H.J.A.; Martinez-Lucio, T.S.; Boersma, H.H.; Borra, R.H.; Cornelissen, B.; Dierckx, R.A.J.O.; Dobrolinska, M.; Doorduin, J.; Erba, P.A.; Glaudemans, A.W.J.M.; et al. [15O]H2O PET: Potential or Essential for Molecular Imaging? *Semin. Nucl. Med.* **2024**, *54*, 761–773, doi:10.1053/j.semnuclmed.2023.08.002.
23. Hobbs, R.F.; Wahl, R.L.; Lodge, M.A.; Javadi, M.S.; Cho, S.Y.; Chien, D.T.; Ewertz, M.E.; Esaias, C.E.; Ladenson, P.W.; Sgouros, G. ^{124} I PET-Based 3D-RD Dosimetry for a Pediatric Thyroid Cancer Patient: Real-Time Treatment Planning and Methodologic Comparison. *J. Nucl. Med.* **2009**, *50*, 1844–1847, doi:10.2967/jnumed.109.066738.
24. Sgouros, G.; Hobbs, R.F.; Atkins, F.B.; Van Nostrand, D.; Ladenson, P.W.; Wahl, R.L. Three-Dimensional Radiobiological Dosimetry (3D-RD) with 124I PET for 131I Therapy of Thyroid Cancer. *Eur. J. Nucl. Med. Mol. Imaging* **2011**, *38*, 41–47, doi:10.1007/s00259-011-1769-1.
25. Pauwels, E.; Cleeren, F.; Bormans, G.; Deroose, C.M. Somatostatin Receptor PET Ligands - the next Generation for Clinical Practice.
26. Khawar, A.; Eppard, E.; Sinnes, J.P.; Roesch, F.; Ahmadzadehfar, H.; Kürpig, S.; Meisenheimer, M.; Gaertner, F.C.; Essler, M.; Bundschuh, R.A. [44Sc]Sc-PSMA-617 Biodistribution and Dosimetry in Patients With Metastatic Castration-Resistant Prostate Carcinoma. *Clin. Nucl. Med.* **2018**, *43*, 323–330, doi:10.1097/RLU.0000000000002003.
27. Krasnovskaya, O.O.; Abramchuck, D.; Erofeev, A.; Gorelkin, P.; Kuznetsov, A.; Shemukhin, A.; Beloglazkina, E.K. Recent Advances in 64Cu/67Cu-Based Radiopharmaceuticals. *Int. J. Mol. Sci.* **2023**, *24*, 9154, doi:10.3390/ijms24119154.
28. Cui, C.; Hanyu, M.; Hatori, A.; Zhang, Y.; Xie, L.; Ohya, T.; Fukada, M.; Suzuki, H.; Nagatsu, K.; Jiang, C.; et al. Synthesis and Evaluation of [64Cu]PSMA-617 Targeted for Prostate-Specific Membrane Antigen in Prostate Cancer.
29. Mojtahedi, A.; Thamake, S.; Tworowska, I.; Ranganathan, D.; Delpassand, E.S. The Value of 68Ga-DOTATATE PET/CT in Diagnosis and Management of Neuroendocrine Tumors Compared to Current FDA Approved Imaging Modalities: A Review of Literature.
30. Carlucci, G.; Ippisch, R.; Slavik, R.; Mishoe, A.; Blecha, J.; Zhu, S. ^{68}Ga-PSMA-11 NDA Approval: A Novel and Successful Academic Partnership. *J. Nucl. Med.* **2021**, *62*, 149–155, doi:10.2967/jnumed.120.260455.
31. Harnett et al. Clinical Performance of Rb-82 Myocardial Perfusion PET and Tc-99m-Based SPECT in Patients with Extreme Obesity.
32. Helisch, A.; Förster, GregorJ.; Reber, H.; Buchholz, H.-G.; Arnold, R.; Göke, B.; Weber, MatthiasM.; Wiedenmann, B.; Pauwels, S.; Haus, U.; et al. Pre-Therapeutic Dosimetry and Biodistribution of 86Y-DOTA-Phe1-Tyr3-Octreotide versus 111In-Pentetreotide in Patients with Advanced Neuroendocrine Tumours. *Eur. J. Nucl. Med. Mol. Imaging* **2004**, *31*, doi:10.1007/s00259-004-1561-6.
33. Laforest, R.; Lapi, S.E.; Oyama, R.; Bose, R.; Tabchy, A.; Marquez-Nostra, B.V.; Burkemper, J.; Wright, B.D.; Frye, J.; Frye, S.; et al. [89Zr]Trastuzumab: Evaluation of Radiation Dosimetry, Safety, and Optimal Imaging Parameters in Women with HER2-Positive Breast Cancer. *Mol. Imaging Biol.* **2016**, *18*, 952–959, doi:10.1007/s11307-016-0951-z.

 doi:10.20944/preprints202604.0617.v1

34. Escorcia, F.E.; Houghton, J.L.; Abdel-Atti, D.; Pereira, P.R.; Cho, A.; Gutsche, N.T.; Baidoo, K.E.; Lewis, J.S. ImmunoPET Predicts Response to Met-Targeted Radioligand Therapy in Models of Pancreatic Cancer Resistant to Met Kinase Inhibitors. *Theranostics* **2020**, *10*, 151–165, doi:10.7150/thno.37098.
35. Kapoor, M.; Heston, T.F.; Kasi, A. PET Scanning. *StatPearls* [Internet]. StatPearls Publishing: Treasure Island (FL), 2026. Available online: https://www.ncbi.nlm.nih.gov/books/NBK559089/.
36. Piel, M.; Vernaleken, I.; Rösch, F. Positron Emission Tomography in CNS Drug Discovery and Drug Monitoring. *J. Med. Chem.* **2014**, *57*, 9232–9258, doi:10.1021/jm5001858.
37. Hauser, A.S.; Attwood, M.M.; Rask-Andersen, M.; Schiöth, H.B.; Gloriam, D.E. Trends in GPCR Drug Discovery: New Agents, Targets and Indications. *Nat. Rev. Drug Discov.* **2017**, *16*, 829–842, doi:10.1038/nrd.2017.178.
38. Whalen, E.J.; Rajagopal, S.; Lefkowitz, R.J. Therapeutic Potential of β-Arrestin- and G Protein-Biased Agonists. *Trends Mol. Med.* **2011**, *17*, 126–139, doi:10.1016/j.molmed.2010.11.004.
39. Sriram, K.; Insel, P.A. G Protein-Coupled Receptors as Targets for Approved Drugs: How Many Targets and How Many Drugs? *Mol. Pharmacol.* **2018**, *93*, 251–258, doi:10.1124/mol.117.111062.
40. Krishna Deepak, R.N.V.; Verma, R.K.; Hartono, Y.D.; Yew, W.S.; Fan, H. Recent Advances in Structure, Function, and Pharmacology of Class A Lipid GPCRs: Opportunities and Challenges for Drug Discovery. *Pharmaceuticals* **2021**, *15*, 12, doi:10.3390/ph15010012.
41. García-Nafría, J.; Tate, C.G. Structure Determination of GPCRs: Cryo-EM Compared with X-Ray Crystallography. *Biochem. Soc. Trans.* **2021**, *49*, 2345–2355, doi:10.1042/BST20210431.
42. Insel, P.A.; Sriram, K.; Gorr, M.W.; Wiley, S.Z.; Michkov, A.; Salmerón, C.; Chinn, A.M. GPCRomics: An Approach to Discover GPCR Drug Targets. *Trends Pharmacol. Sci.* **2019**, *40*, 378–387, doi:10.1016/j.tips.2019.04.001.
43. Feng, C.; Ooms, J.F.; Danen, E.H.J.; Heitman, L.H. GPCR-G Protein Signalling and Its Mutational Landscape in Cancer—Driver or Passenger. *Br. J. Pharmacol.* **2025**, *182*, 3975–3989, doi:10.1111/bph.70102.
44. O'Hayre, M.; Degese, M.S.; Gutkind, J.S. Novel Insights into G Protein and G Protein-Coupled Receptor Signaling in Cancer. *Curr. Opin. Cell Biol.* **2014**, *27*, 126–135, doi:10.1016/j.ceb.2014.01.005.
45. Insel, P.A.; Sriram, K.; Wiley, S.Z.; Wilderman, A.; Katakia, T.; McCann, T.; Yokouchi, H.; Zhang, L.; Corriden, R.; Liu, D.; et al. GPCRomics: GPCR Expression in Cancer Cells and Tumors Identifies New, Potential Biomarkers and Therapeutic Targets. *Front. Pharmacol.* **2018**, *9*, 431, doi:10.3389/fphar.2018.00431.
46. Møller, L.N.; Stidsen, C.E.; Hartmann, B.; Holst, J.J. Somatostatin Receptors. *Biochim. Biophys. Acta BBA - Biomembr.* **2003**, *1616*, 1–84, doi:10.1016/S0005-2736(03)00235-9.
47. Theodoropoulou, M.; Stalla, G.K. Somatostatin Receptors: From Signaling to Clinical Practice. *Front. Neuroendocrinol.* **2013**, *34*, 228–252, doi:10.1016/j.yfrne.2013.07.005.
48. Mikołajczak, R.; Maecke, H.R. Radiopharmaceuticals for Somatostatin Receptor Imaging. *Nucl. Med. Rev.* **2016**, *19*, 126–132, doi:10.5603/NMR.2016.0024.
49. Kwekkeboom, D.; Krenning, E.P.; de Jong, M. Peptide Receptor Imaging and Therapy.
50. Zhao, J.; Zhu, Y.; Chen, M. Somatostatin Subtype-2 Receptor (SST2R) Targeted Therapeutics and Uses Thereof. US20240254106, (2024).
51. Oron-Herman, M.; Kirmayer, D.; Lupp, A.; Schulz, S.; Kostenich, G.; Afargan, M. Expression Prevalence and Dynamics of GPCR Somatostatin Receptors 2 and 3 as Cancer Biomarkers beyond NET: A Paired Immunohistochemistry Approach. *Sci. Rep.* **2023**, *13*, 20857, doi:10.1038/s41598-023-47877-0.
52. Afargan, M.; Blum, E.; Salitra, Y. Conformational Constrained Somatostatin Receptor 3 Peptide Ligands and Their Conjugates and Uses Thereof. US20240165282, (2024).
53. Rottenburger, C.; Nicolas, G.P.; McDougall, L.; Kaul, F.; Cachovan, M.; Vija, A.H.; Schibli, R.; Geistlich, S.; Schumann, A.; Rau, T.; et al. Cholecystokinin 2 Receptor Agonist^{177} Lu-PP-F11N for Radionuclide Therapy of Medullary Thyroid Carcinoma: Results of the Lumed Phase 0a Study. *J. Nucl. Med.* **2020**, *61*, 520–526, doi:10.2967/jnumed.119.233031.
54. Pokorska-Bocci, A.; Attinger, A. Method for Predicting the Response of a Patient Diagnosed with Cancer to Treatment and/or Imaging with a Compound Targeting CCK2-R, and Compound for Use in Methods of Selectively Treating and/or Imaging Cancer. US20240401145, (2024).

 doi:10.20944/preprints202604.0617.v1

55. Behe, Martin; Schibli, Roger Mini-Gastrin Analogue, in Particular for Use in CCK2 Receptor Positive Tumour Diagnosis and/or Treatment. WO2015067473, (2015).
56. Levy, F.; Attinger, A. Gallium-Labeled Gastrin Analogue and Use in a Method of Imaging CCKB-Receptor-Positive Tumors or Cancers. US20230270893, (2023).
57. Liu, F.; Hu, T. Dual Receptor Targeting Radioligands and Uses Thereof. WO2024083224, (2024).
58. Zou, Y.-R.; Kottmann, A.H.; Kuroda, M.; Taniuchi, I.; Littman, D.R. Function of the Chemokine Receptor CXCR4 in Haematopoiesis and in Cerebellar Development. *Nature* **1998**, *393*, 595–599, doi:10.1038/31269.
59. Jacobson, O.; Weiss, I.D. CXCR4 Chemokine Receptor Overview: Biology, Pathology and Applications in Imaging and Therapy. *Theranostics* **2013**, *3*, 1–2, doi:10.7150/thno.5760.
60. Yu, J.; Zhou, X.; Shen, L. CXCR4-Targeted Radiopharmaceuticals for the Imaging and Therapy of Malignant Tumors. *Molecules* **2023**, *28*, 4707, doi:10.3390/molecules28124707.
61. Amodeo, P.; Vitale, R.; De Luca, S.; Scala, S.; Castello, G.; Siani, A. Cyclic Peptides Binding CXCR4 Receptor and Relative Medical and Diagnostic Uses. WO2011092575, (2011).
62. Scala, S.; Trotta, A.M. Radiolabeled Peptides for Non-Invasive Diagnosis and Treatment of CXCR4 Expressing Tumors. WO2021130329, (2021).
63. Di Maro, S.; Di Leva, F.S.; Trotta, A.M.; Brancaccio, D.; Portella, L.; Aurilio, M.; Tomassi, S.; Messere, A.; Sementa, D.; Lastoria, S.; et al. Structure–Activity Relationships and Biological Characterization of a Novel, Potent, and Serum Stable C-X-C Chemokine Receptor Type 4 (CXCR4) Antagonist. *J. Med. Chem.* **2017**, *60*, 9641–9652, doi:10.1021/acs.jmedchem.7b01062.
64. Garcia-Recio, S.; Gascón, P. Biological and Pharmacological Aspects of the NK1-Receptor. *BioMed Res. Int.* **2015**, *2015*, 1–14, doi:10.1155/2015/495704.
65. Ebrahimi, S.; Mirzavi, F.; Aghaee-Bakhtiari, S.H.; Hashemy, S.I. SP/NK1R System Regulates Carcinogenesis in Prostate Cancer: Shedding Light on the Antitumoral Function of Aprepitant. *Biochim. Biophys. Acta BBA - Mol. Cell Res.* **2022**, *1869*, 119221, doi:10.1016/j.bbamcr.2022.119221.
66. Tattersall, F.D.; Rycrofti, W.; Francis, B.; PEARCEl, D.; Merchant', K.; MacLEODl, A.M.; SWAINl, C.; BAKERl, R.; Ber', E.; Metzger, J.; et al. Tachykinin NK1 Receptor Antagonists Act Centrally to Inhibit Ernesis Induced by the Chemotherapeutic Agent Cisplatin in Ferrets.
67. Nestor, Marika; Bengtsson, Christoffer; Yngve, Ulrika; Begnini, Fabio; Jha, Preeti; Rosenström, Ulrika Substituted 2-Phenylpiperidine Compounds for Use in the Diagnosis, Treatment and/or Prevention of Cancer. WO2025008409, (2025).
68. Fridmanis, D.; Roga, A.; Klovins, J. ACTH Receptor (MC2R) Specificity: What Do We Know About Underlying Molecular Mechanisms? *Front. Endocrinol.* **2017**, *8*, doi:10.3389/fendo.2017.00013.
69. Zhao, J.; Chen, M.; Zhu, Y.; Kim, S.H. Melanocortin Type 2 Receptor (MC2R) Targeted Therapeutics and Uses Thereof. US20230405157, (2023).
70. Kirby, H.R.; Maguire, J.J.; Colledge, W.H.; Davenport, A.P. International Union of Basic and Clinical Pharmacology. LXXVII. Kisspeptin Receptor Nomenclature, Distribution, and Function. *Pharmacol. Rev.* **2010**, *62*, 565–578, doi:10.1124/pr.110.002774.
71. Navarro, V.M.; Castellano, J.M.; McConkey, S.M.; Pineda, R.; Ruiz-Pino, F.; Pinilla, L.; Clifton, D.K.; Tena-Sempere, M.; Steiner, R.A. Interactions between Kisspeptin and Neurokinin B in the Control of GnRH Secretion in the Female Rat. *Am. J. Physiol.-Endocrinol. Metab.* **2011**, *300*, E202–E210, doi:10.1152/ajpendo.00517.2010.
72. Curtis, A.E.; Cooke, J.H.; Baxter, J.E.; Parkinson, J.R.C.; Bataveljic, A.; Ghatei, M.A.; Bloom, S.R.; Murphy, K.G. A Kisspeptin-10 Analog with Greater in Vivo Bioactivity than Kisspeptin-10. *Am. J. Physiol.-Endocrinol. Metab.* **2010**, *298*, E296–E303, doi:10.1152/ajpendo.00426.2009.
73. Rodríguez Sarmiento, D.Y. Beyond Reproduction: Exploring the Non-Canonical Roles of the Kisspeptin System in Diverse Biological Systems. *Bionatura* **2023**, *8*, 1–6, doi:10.21931/RB/2023.08.03.13.
74. Rodríguez-Sarmiento, D.Y.; Rondón-Villarreal, P.; Scarpelli-Pereira, P.H.; Bouvier, M. Comprehensive Analysis of Kisspeptin Signaling: Effects on Cellular Dynamics in Cervical Cancer. *Biomolecules* **2024**, *14*, 923, doi:10.3390/biom14080923.
75. Liu, Junjie; Zhu, Yunfei; Xiong, Yifeng Kisspeptin Receptor (KISS1R) Targeted Therapeutics and Uses Thereof. WO2024206577, (2024).

 doi:10.20944/preprints202604.0617.v1

76. Vincent, J.-P.; Mazella, J.; Kitabgi, P. Neurotensin and Neurotensin Receptors. *Trends Pharmacol. Sci.* **1999**, *20*, 302–309, doi:10.1016/S0165-6147(99)01357-7.
77. Vincent, J.-P. Neurotensin Receptors: Binding Properties, Transduction Pathways, and Structure. *Cell. Mol. Neurobiol.* **1995**, *15*, 501–512, doi:10.1007/BF02071313.
78. Ehlers, R.A.; Kim, S.; Zhang, Y.; Ethridge, R.T.; Murrilo, C.; Hellmich, M.R.; Evans, D.B.; Townsend, C.M.; Mark Evers, B. Gut Peptide Receptor Expression in Human Pancreatic Cancers: *Ann. Surg.* **2000**, *231*, 838–848, doi:10.1097/00000658-200006000-00008.
79. Gui, X.; Guzman, G.; Dobner, P.R.; Kadkol, S.S. Increased Neurotensin Receptor-1 Expression during Progression of Colonic Adenocarcinoma. *Peptides* **2008**, *29*, 1609–1615, doi:10.1016/j.peptides.2008.04.014.
80. Souazé, F.; Dupouy, S.; Viardot-Foucault, V.; Bruyneel, E.; Attoub, S.; Gespach, C.; Gompel, A.; Forgez, P. Expression of Neurotensin and NT1 Receptor in Human Breast Cancer: A Potential Role in Tumor Progression. *Cancer Res.* **2006**, *66*, 6243–6249, doi:10.1158/0008-5472.CAN-06-0450.
81. Dupouy, S.; Viardot-Foucault, V.; Alifano, M.; Souazé, F.; Plu-Bureau, G.; Chaouat, M.; Lavaur, A.; Hugol, D.; Gespach, C.; Gompel, A.; et al. The Neurotensin Receptor-1 Pathway Contributes to Human Ductal Breast Cancer Progression. *PLoS ONE* **2009**, *4*, e4223, doi:10.1371/journal.pone.0004223.
82. Baum, R.P.; Singh, A.; Schuchardt, C.; Kulkarni, H.R.; Klette, I.; Wiessalla, S.; Osterkamp, F.; Reineke, U.; Smerling, C. ^{177} Lu-3BP-227 for Neurotensin Receptor 1–Targeted Therapy of Metastatic Pancreatic Adenocarcinoma: First Clinical Results. *J. Nucl. Med.* **2018**, *59*, 809–814, doi:10.2967/jnumed.117.193847.
83. D Gully Biochemical and Pharmacological Activities of SR 142948A, a New Potent Neurotensin Receptor Antagonist. *The Journal of pharmacology and experimental therapeutics* **1997**, *280*.
84. Liu, F. Compounds and Radioligands for Targeting Neurotensin Receptor and Uses Thereof. US20240287046, (2024).
85. Savoie, F.-A.; Arpin, D.J.; Vaillancourt, D.E. Magnetic Resonance Imaging and Nuclear Imaging of ParkinsonianDisorders: Where Do We Go from Here? *Curr. Neuropharmacol.* **2024**, *22*, 1583–1605, doi:10.2174/1570159X21666230801140648.
86. Xie, L.; Zhao, J.; Li, Y.; Bai, J. PET Brain Imaging in Neurological Disorders. *Phys. Life Rev.* **2024**, *49*, 100–111, doi:10.1016/j.plrev.2024.03.007.
87. Doroszkiewicz, J.; Groblewska, M.; Mroczko, B. Molecular Biomarkers and Their Implications for the Early Diagnosis of Selected Neurodegenerative Diseases. *Int. J. Mol. Sci.* **2022**, *23*, 4610, doi:10.3390/ijms23094610.
88. Colom, M.; Vidal, B.; Zimmer, L. Is There a Role for GPCR Agonist Radiotracers in PET Neuroimaging? *Front. Mol. Neurosci.* **2019**, *12*, 255, doi:10.3389/fnmol.2019.00255.
89. Kew, J.N.C.; Kemp, J.A. Ionotropic and Metabotropic Glutamate Receptor Structure and Pharmacology. *Psychopharmacology (Berl.)* **2005**, *179*, 4–29, doi:10.1007/s00213-005-2200-z.
90. P. Jeffrey Conn; Jean-Philippe Pin. Pharmacology and Functions of Metabotropic Glutamate Receptors. **1997**, *37*, doi:10.1146/annurev.pharmtox.37.1.205.
91. Cartmell, J.; Schoepp, D.D. Regulation of Neurotransmitter Release by Metabotropic Glutamate Receptors. *J. Neurochem.* **2000**, *75*, 889–907, doi:10.1046/j.1471-4159.2000.0750889.x.
92. Conn, P.J.; Lindsley, C.W.; Jones, C.K. Activation of Metabotropic Glutamate Receptors as a Novel Approach for the Treatment of Schizophrenia. *Trends Pharmacol. Sci.* **2009**, *30*, 25–31, doi:10.1016/j.tips.2008.10.006.
93. Andrés-Gil, J.I.; Gool, M.L.M.V.; Bormans, G.M.R.; Verbeek, J. Radiolabelled mGluR2/3 PET Ligands. US20200306389, (2020).
94. Leurquin-Sterk, G.; Celen, S.; Van Laere, K.; Koole, M.; Bormans, G.; Langlois, X.; Van Hecken, A.; Te Riele, P.; Alcázar, J.; Verbruggen, A.; et al. What We Observe In Vivo Is Not Always What We See In Vitro: Development and Validation of^{11} C-JNJ-42491293, A Novel Radioligand for mGluR2. *J. Nucl. Med.* **2017**, *58*, 110–116, doi:10.2967/jnumed.116.176628.
95. Yuan, Gengyang; Brownell, Anna-Liisa Chromane Imaging Ligands. WO2023278729, (2023).
96. Gool, M.L., Maria Van; Andrés-Gil, J.I.; Alcázar-Vaca, M.J.; Bormans, G.M.R.; Celen, S.J.L.; Verbeek, J. Radiolabelled mGluR2 PET Ligands. US20210177995, (2021).
97. Zhang, Z.; Zheng, B.; Yuan, G.; Neelamegam, R.; Brownell, A.-L. Modulators of Metabotropic Glutamate Receptor 2. US20210246140, (2021).

 doi:10.20944/preprints202604.0617.v1

98. Zhang, Z.; Wang, J.; Shoup, T.M.; Brownell, A.-L. Modulators of Metabotropic Glutamate Receptor 4. US20220118117, (2022).
99. J W Kebabian Multiple Classes of Dopamine Receptors in Mammalian Central Nervous System: The Involvement of Dopamine-Sensitive Adenylyl Cyclase.
100. Beaulieu, J.-M.; Gainetdinov, R.R. The Physiology, Signaling, and Pharmacology of Dopamine Receptors. *Pharmacol. Rev.* **2011**, *63*, 182–217, doi:10.1124/pr.110.002642.
101. J K Wamsley; D R Gehlert; F M Filloux; T M Dawson Comparison of the Distribution of D-1 and D-2 Dopamine Receptors in the Rat Brain. *J Chem Neuroanat* **1989**.
102. Marc Savasta; Alain Dubois; Bernard Scätton Autoradiographic Localization of D1 Dopamine Receptors in the Rat Brain with [3H]SCH 23390. *Brain Res* **1986**, *375*, doi:10.1016/0006-8993(86)90749-3.
103. Chihiro Yokoyama; Hitoshi Okamura; Teruo Nakajima; Jun-Ichi Taguchi; Yasuhiko Ibata Autoradiographic Distribution of [3H]YM-09151-2, a High-Affinity and Selective Antagonist Ligand for the Dopamine D2 Receptor Group, in the Rat Brain and Spinal Cord. *J Comp Neurol* **1994**, doi:https://doi.org/10.1002/cne.903440109Digital Object Identifier (DOI).
104. Prante, O.; Maschauer, S.; Banerjee, A. Radioligands for the Dopamine Receptor Subtypes. *J. Label. Compd. Radiopharm.* **2013**, *56*, 130–148, doi:10.1002/jlcr.3000.
105. Mercier, J.; Valade, A.; Vermeiren, C.; Wood, M.; Macquire, R. Imaging Agents. US20240343737, (2024).
106. MacRitchie, N.; Frleta-Gilchrist, M.; Sugiyama, A.; Lawton, T.; McInnes, I.B.; Maffia, P. Molecular Imaging of Inflammation - Current and Emerging Technologies for Diagnosis and Treatment. *Pharmacol. Ther.* **2020**, *211*, 107550, doi:10.1016/j.pharmthera.2020.107550.
107. Calabria, F.F.; Guadagnino, G.; Cimini, A.; Leporace, M. PET/CT Imaging of Infectious Diseases: Overview of Novel Radiopharmaceuticals. *Diagnostics* **2024**, *14*, 1043, doi:10.3390/diagnostics14101043.
108. Glaudemans, A.W.J.M.; De Vries, E.F.J.; Galli, F.; Dierckx, R.A.J.O.; Slart, R.H.J.A.; Signore, A. The Use of 18 F-FDG-PET/CT for Diagnosis and Treatment Monitoring of Inflammatory and Infectious Diseases. *Clin. Dev. Immunol.* **2013**, *2013*, 1–14, doi:10.1155/2013/623036.
109. Wiehr, S.; Warnke, P.; Rolle, A.-M.; Schütz, M.; Oberhettinger, P.; Kohlhofer, U.; Quintanilla-Martinez, L.; Maurer, A.; Thornton, C.; Boschetti, F.; et al. New Pathogen-Specific immunoPET/MR Tracer for Molecular Imaging of a Systemic Bacterial Infection. *Oncotarget* **2016**, *7*, 10990–11001, doi:10.18632/oncotarget.7770.
110. Mulero, F. Editorial: ImmunoPET Imaging in Disease Diagnosis and Therapy Assessment. *Front. Med.* **2023**, *10*, 1231525, doi:10.3389/fmed.2023.1231525.
111. Sun, L.; Ye, R.D. Role of G Protein-Coupled Receptors in Inflammation. *Acta Pharmacol. Sin.* **2012**, *33*, 342–350, doi:10.1038/aps.2011.200.
112. Liu, Y.; Gropler, R.; Brody, S.; Kreisel, D. Methods for Detecting CCR2 Receptors. US20200405889, (2020).
113. Scholten, D.; Canals, M.; Maussang, D.; Roumen, L.; Smit, M.; Wijtmans, M.; De Graaf, C.; Vischer, H.; Leurs, R. Pharmacological Modulation of Chemokine Receptor Function. *Br. J. Pharmacol.* **2012**, *165*, 1617–1643, doi:10.1111/j.1476-5381.2011.01551.x.
114. Uhlén, M.; Fagerberg, L.; Hallström, B.M.; Lindskog, C.; Oksvold, P.; Mardinoglu, A.; Sivertsson, Å.; Kampf, C.; Sjöstedt, E.; Asplund, A.; et al. Tissue-Based Map of the Human Proteome. *Science* **2015**, *347*, 1260419, doi:10.1126/science.1260419.
115. Philip M. Murphy; H. Lee Tiffany Cloning of Complementary DNA Encoding a Functional Human Interleukin-8 Receptor. *Science* **1991**, *253*, doi:10.1126/science.1891716.
116. Decker, Michael; Higuchi, Takahiro; Spatz, Philipp ^{18}F-CXCR2 PETtracer. WO2025149577, (2025).
117. Nanki, T.; Hayashida, K.; El-Gabalawy, H.S.; Suson, S.; Shi, K.; Girschick, H.J.; Yavuz, S.; Lipsky, P.E. Stromal Cell-Derived Factor-1-CXC Chemokine Receptor 4 Interactions Play a Central Role in CD4+ T Cell Accumulation in Rheumatoid Arthritis Synovium. *J. Immunol.* **2000**, *165*, 6590–6598, doi:10.4049/jimmunol.165.11.6590.
118. Bot, I.; Daissormont, I.T.M.N.; Zernecke, A.; Van Puijvelde, G.H.M.; Kramp, B.; De Jager, S.C.A.; Sluimer, J.C.; Manca, M.; Hérias, V.; Westra, M.M.; et al. CXCR4 Blockade Induces Atherosclerosis by Affecting Neutrophil Function. *J. Mol. Cell. Cardiol.* **2014**, *74*, 44–52, doi:10.1016/j.yjmcc.2014.04.021.
119. Bénard, F.; Lin, K.-S.; Rousseau, E.; Zhang, Z.; Kwon, D.; Lau, J.; Munoz, C.U.; Lozada, J.; Perrin, D. Novel Radiolabelled CXCR4-Targeting Compounds for Diagnosis and Therapy. US20220218852, (2022).

 doi:10.20944/preprints202604.0617.v1

120. Bénard, François; Lin, Kuo-Shyan; Zhang, Zhengxing; Kwon, Daniel; Perrin, David; Todorovic, Mihajlo; Lozada, Jerome; Li, Lee Lee Novel CXCR4-Targeting Compounds. WO2022082312, (2022).
121. James, Michelle L.; Jackson, Isaac M.; Kalita, Mausam; Nagy, Sydney C. Method for Detecting Innate Immune Action in Vivo Using GPR84-PET. WO2024220480, (2024).
122. Labéguère, F.; Dupont, S.; Alvey, L.; Soulas, F.; Newsome, G.; Tirera, A.; Quenehen, V.; Mai, T.T.T.; Deprez, P.; Blanqué, R.; et al. Discovery of 9-Cyclopropylethynyl-2-((*S*)-1-[1,4]Dioxan-2-Ylmethoxy)-6,7-Dihydropyrimido[6,1- *a*]Isoquinolin-4-One (GLPG1205), a Unique GPR84 Negative Allosteric Modulator Undergoing Evaluation in a Phase II Clinical Trial. *J. Med. Chem.* **2020**, *63*, 13526–13545, doi:10.1021/acs.jmedchem.0c00272.
123. Zhou, H.; Chen, Z.; Gao, S.; Lian, C.; Hu, J.; Lu, J.; Zhang, L. GPR65 Is a Novel Immune Biomarker and Regulates the Immune Microenvironment in Lung Adenocarcinoma. *Front. Immunol.* **2025**, *16*, 1572757, doi:10.3389/fimmu.2025.1572757.